NAVAL POSTGRADUATE SCHOOL
Monterey, California

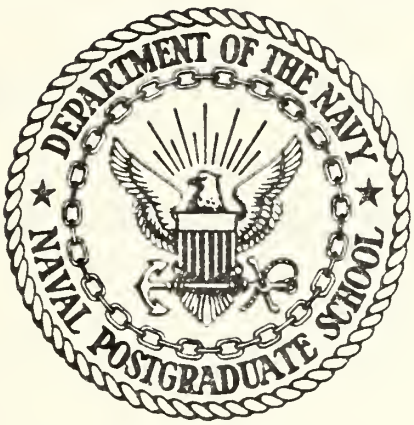

THESIS

GRAVITATIONAL EFFECTS ON THE OPERATION
OF
A VARIABLE CONDUCTANCE HEAT PIPE

by

Robert Scott Owendoff

March 1977

Thesis Advisor: M. D. Kelleher

Approved for public release; distribution unlimited.

SECURITY CLASSIFICATION OF THIS PAGE (When Data Entered)

REPORT DOCUMENTATION PAGE

READ INSTRUCTIONS BEFORE COMPLETING FORM

1. REPORT NUMBER	2. GOVT ACCESSION NO. / 3. RECIPIENT'S CATALOG NUMBER
4. TITLE (and Subtitle): Gravitational Effects on the Operation of a Variable Conductance Heat Pipe	5. TYPE OF REPORT & PERIOD COVERED: Master's Thesis; March 1977
	6. PERFORMING ORG. REPORT NUMBER
7. AUTHOR(s): Robert Scott Owendoff	8. CONTRACT OR GRANT NUMBER(s)
9. PERFORMING ORGANIZATION NAME AND ADDRESS: Naval Postgraduate School, Monterey, CA 93940	10. PROGRAM ELEMENT, PROJECT, TASK AREA & WORK UNIT NUMBERS
11. CONTROLLING OFFICE NAME AND ADDRESS: Naval Postgraduate School, Monterey, CA 93940	12. REPORT DATE: March 1977
	13. NUMBER OF PAGES: 74
14. MONITORING AGENCY NAME & ADDRESS (if different from Controlling Office): Naval Postgraduate School, Monterey, CA 93940	15. SECURITY CLASS. (of this report): Unclassified
	15a. DECLASSIFICATION/DOWNGRADING SCHEDULE

16. DISTRIBUTION STATEMENT (of this Report)

Approved for public release; distribution unlimited.

17. DISTRIBUTION STATEMENT (of the abstract entered in Block 20, if different from Report)

18. SUPPLEMENTARY NOTES

19. KEY WORDS (Continue on reverse side if necessary and identify by block number)

Heat pipe
Heat transfer device
Gas loaded heat pipe
Variable conductance heat pipe

20. ABSTRACT (Continue on reverse side if necessary and identify by block number)

A variable conductance heat pipe, measuring 2.5 centimeters in diameter and 152 centimeters in length, was built. The heat pipe was operated in both the conventional and variable conductance modes to obtain experimental data concerning performance characteristics. The input electrical power was varied from 20 to 50 watts with the heat pipe placed in both the horizontal and vertical positions. Methanol and Freon 113 were selected as the working fluids; helium and krypton were the non-condensible gases. In the variable

DD FORM 1 JAN 73 1473 EDITION OF 1 NOV 65 IS OBSOLETE
S/N 0102-014-6601 |

SECURITY CLASSIFICATION OF THIS PAGE (When Data Entered)

conductance mode, liquid crystals were used to observe qualitatively the temperature gradients occurring across the vapor-gas interface. Summarized performance data for the various operating conditions and graphs of the isotherms obtained from the liquid crystal data are presented.

conductance mode, liquid crystals were used to observe qualitatively the temperature gradients occurring across the vapor-gas interface. Summarized performance data for the various operating conditions and graphs of the isotherms obtained from the liquid crystal data are presented.

Approved for public release; distribution unlimited.

Gravitational Effects on the Operation of a Variable Conductance Heat Pipe

by

Robert Scott Owendoff
Lieutenant, United States Navy
B.S., United States Naval Academy, 1968

Submitted in partial fulfillment of the
requirements for the degree of

MASTER OF SCIENCE IN MECHANICAL ENGINEERING

from the

NAVAL POSTGRADUATE SCHOOL
March 1977

ABSTRACT

A variable conductance heat pipe, measuring 2.5 centimeters in diameter and 152 centimeters in length, was built. The heat pipe was operated in both the conventional and variable conductance modes to obtain experimental data concerning performance characteristics. The input electrical power was varied from 20 to 50 watts with the heat pipe placed in both the horizontal and vertical positions. Methanol and Freon 113 were selected as the working fluids; helium and krypton were the non-condensible gases. In the variable conductance mode, liquid crystals were used to observe qualitatively the temperature gradients occurring across the vapor-gas interface. Summarized performance data for the various operating conditions and graphs of the isotherms obtained from the liquid crystal data are presented.

TABLE OF CONTENTS

LIST OF TABLES

LIST OF FIGURES

ACKNOWLEDGEMENTS

The author wishes to thank sincerely the several people who made this experiment successful. However, since it is impossible to acknowledge everyone, it is hoped that those unnamed persons will nevertheless be aware of the author's appreciation for their assistance.

Mr. George Bixler performed very competently in fabricating the heat pipe components and offered many helpful suggestions. Mr. Thomas Christian was excellent in doing the required electrical work as well as quickly rectifying instrumentation malfunctions when they occurred.

Lastly and foremost, Professor Matthew Kelleher was indeed the guiding light in this experiment. Without his expert guidance and support, this research would not have been completed.

I. INTRODUCTION

A. BACKGROUND

The heat pipe is a high performance heat transmission device. Experiments have shown the heat pipe's ability to conduct heat 1,000 to 10,000 times more effectively than the same size solid rod [Ref. 1]. Although the principle of the heat pipe was first proposed by Gaugler in 1942 [Ref. 2], Grover [Ref. 3] and his colleagues at the Los Alamos Scientific Laboratory did the pioneer developmental work in the early 1960's. Since that time a significant amount of research has been done in this field, resulting in over one thousand papers having been published on this subject. Simplicity of construction, flexibility, ease of control, and ability to transport heat at a high rate over a considerable distance with a small temperature drop are some of the many outstanding advantages of using the heat pipe as a heat transmission device. The numerous heat pipe applications range from cooling of electronic equipment, solar collectors, engine heating and cooling, surgery cyroprobes, and cooling of space vehicles to permafrost stabilizers for the trans-Alaskan pipeline. References 4, 5, and 6 contain excellent presentations on the theory and design of heat pipes as well as extensive bibliographies. Variable conductance heat pipes are especially well-described in Reference 6.

B. CONVENTIONAL HEAT PIPE

In its simplest form, the heat pipe is a closed cylinder whose inner surface is lined with a porous capillary wick. The liquid phase

of a working fluid saturates the wick with the remaining volume being occupied by the vapor phase of the working fluid. In operation, an external heat source vaporizes the working fluid at the heated or evaporator section of the heat pipe (Figure 1). The resulting pressure difference drives the vapor along the pipe to the opposite or condenser section where the vapor condenses releasing its latent heat of vaporization to a heat sink. Capillary pressure pumps the condensed liquid through the wick back to the evaporator for re-evaporation. Thus, the heat pipe is continuously transporting the latent heat of vaporization from the evaporator to the condenser without wick dry-out occurring. The heat pipe is such an effective heat transfer device because the amount of heat that can be transported as latent heat of vaporization is usually several orders of magnitude greater than that which can be transferred as sensible heat in a conventional convective system. This basic heat pipe operates at essentially isothermal conditions because of the working fluid's phase changes as it travels the length of the heat pipe.

C. VARIABLE CONDUCTANCE HEAT PIPE

The variable conductance heat pipe has the unique feature of being able to maintain the heat source located at its evaporator section at a nearly constant temperature, independent of the power being supplied to the heat source. A conventional heat pipe can be transformed into the basic variable conductance heat pipe by adding a non-condensible gas to the working fluid. The heat pipe operates as previously described, except that the non-condensible gas is swept by the vapor to the condenser end. Since the control gas is non-condensible, it forms a plug at the condenser end (Figure 2). This plug effectively reduces

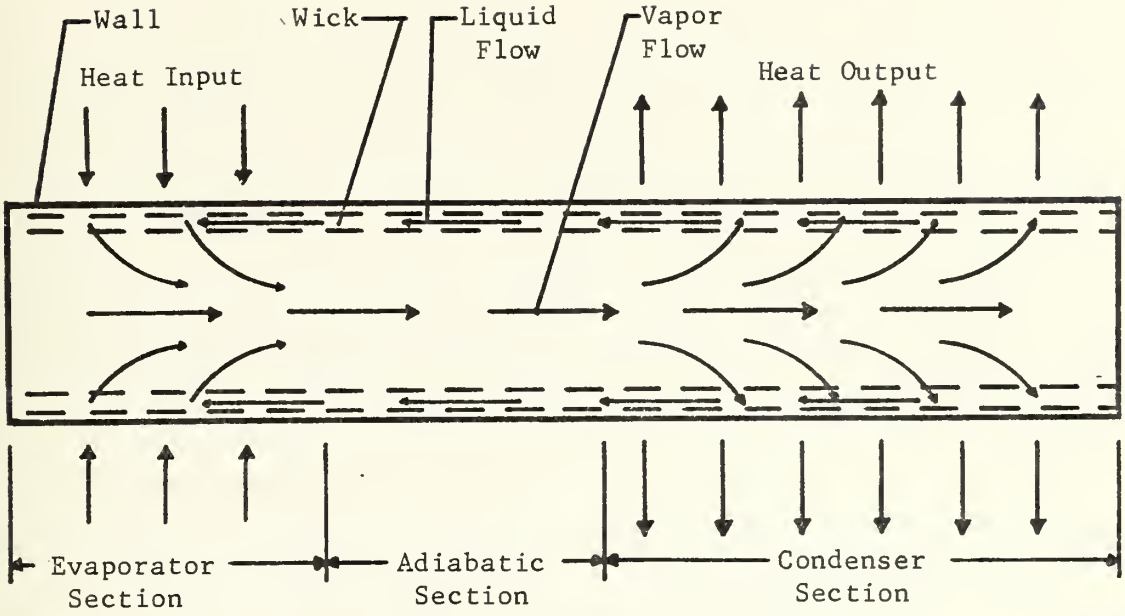

Conventional Heat Pipe Operating Diagram

Figure 1

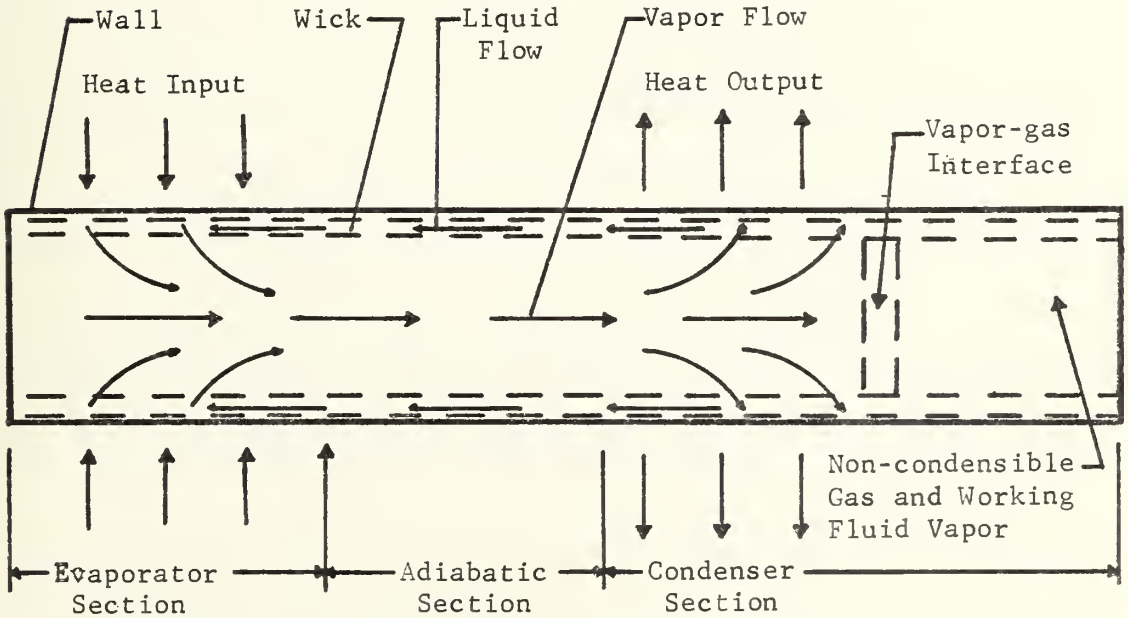

Variable Conductance Heat Pipe Operating Diagram

Figure 2

the condenser length and, therefore, the condenser heat transfer area. As power to the heat source increases, the evaporator temperature rises. This temperature rise causes an increase in the temperature and partial pressure of the working fluid vapor, which compresses the plug of non-condensible gas. Hence, the condenser heat transfer area and the heat pipe conductance are increased, and the system temperature rise is reduced. When the evaporator temperature falls, the vapor pressure of the working fluid drops, and the non-condensible gas volume increases thus blocking a larger portion of the condenser. The net effect of the non-condensible gas is to provide a passively-controlled variable condenser area which increases or decreases with the heat pipe evaporator heat load. As a result, the variable conductance heat pipe has a significantly smaller operating temperature range than the conventional heat pipe for the same power changes to the heat source. This variable conductance characteristic has proven to be most useful in many heat pipe applications.

The simplest mathematical model for analyzing the variable conductance heat pipe is termed the flat front theory originated by Bienert [Ref. 7]. This model makes the following assumptions [Ref. 6]: The conditions in the heat pipe are steady-state, the vapor-gas mixture behaves as an ideal gas, the axial conduction is neglected, the vapor-gas interface is infinitely narrow and perpendicular to the heat pipe axis, the total pressure is uniform throughout the pipe length, and the heat transfer per unit area of the condenser is proportional to the temperature difference between the vapor and heat sink. However, experimental results have shown the vapor-gas interface to be diffuse, and hence the flat front model is inaccurate in predicting the vapor-gas interface.

The diffuse front theory proposed by Marcus [Ref. 6] provides a more realistic model. This one-dimensional model takes into account the important effects of axial conduction and binary mass diffusion between the non-condensible gas and vapor. A computer program using this model was developed to predict the important gas-loaded heat pipe parameters, such as the wall temperature profile along the pipe length and the heat and mass transfer along the pipe. Rohani and Tien [Ref. 8] have modified Marcus' diffuse front model to a two-dimensional theory and developed a computer program to predict the aforementioned heat pipe parameters. They contend that Marcus' one-dimensional model is not sufficient, in many cases, to calculate accurately these two heat pipe parameters.

None of the mathematical models published to date have taken gravitational forces into account for predicting the important heat pipe parameters, such as the wall temperature profile along the pipe length, and, more specifically, the nature of the vapor-gas interface. Naydan [Ref. 9] and Batts [Ref. 10] showed that the vapor-gas interface is appreciably affected by gravity when the molecular weights of the vapor and non-condensible gas are markedly different. They concluded that the diffuse front theory needs to be modified by taking gravity into account when designing a heat pipe for the aforementioned vapor-gas conditions.

II. OBJECTIVE

The objective of this research was to investigate further how gravitational forces would affect the operating characteristics of a variable conductance heat pipe. A heat pipe with a length/diameter ratio of approximately 60:1 was operated at various power levels in both the horizontal and vertical positions. The heat pipe was loaded with non-condensible gases which had molecular weights both greater and less than that of the working fluid. The experimental data should provide further information on the nature and orientation of the vapor-gas interface.

III. EXPERIMENTAL APPARATUS

A. HEAT PIPE CONSTRUCTION

The design objective was to construct a gas-loaded variable conductance heat pipe with a length/diameter ratio of approximately 60 to 1. Previous work has been done by Naydon [Ref. 9] and Batts [Ref. 10] on a variable conductance heat pipe with a length/diameter ratio of about 30 to 1 and by Humphreys [Ref. 11] on a high length/diameter ratio (100 to 1). To complement this earlier work, it was decided to observe the vapor-gas interface on an intermediate length/diameter ratio heat pipe - 60 to 1, in this instance.

Since the heat pipe apparatus built by Naydan proved very successful in operation and a thesis objective was to use Naydan's and Batts' results as a basis of comparison, the heat pipe constructed was very similar to the heat pipe built by Naydan. The pertinent design criteria utilized in this heat pipe construction are the same ones which are described in detail by Naydan.

The heat pipe itself was made from type 304 stainless steel tubing with the following dimensions: length, 152 cm; diameter, 2.5 cm; and wall thickness, 0.051 cm. The wick material was one-hundred-twenty-mesh stainless steel woven wire cloth. Four layers of the wick were held firmly against the inside pipe wall by a stainless steel coil spring. The evaporator and adiabatic sections were 30.5 and 15.2 centimeters in length, respectively.

The condenser end of the heat pipe had a welded stainless steel end cap. Protruding from the center of the end cap was a 0.64-centimeter stainless steel tube which was welded near one end of a fabricated brass cylinder. A pressure transducer was threaded into the other end of the brass cylinder (Figure 3). The brass cylinder was internally ported between the pressure transducer and stainless steel tube connections so that the pressure transducer would measure the pressure at the condenser end of the heat pipe. This assembly was fabricated so that the pressure transducer was mounted evenly with the end of the heat pipe to preclude erroneous pressure readings caused by a height difference between the pressure transducer and the end of the heat pipe. A bleed device was installed on the pressure transducer end of the brass cylinder to bleed any undesirable air from the heat pipe. A small hole was drilled slightly off center in the end cap to house a stainless steel sheated thermocouple that measured the internal heat pipe temperature existing near the condenser end cap.

The evaporator end of the heat pipe had a flanged end plate. One flange face was welded to the heat pipe itself. Both faces were grooved to accommodate an O-ring which sealed both flange faces when the four bolts holding the flange faces together were tightened. The installation of the pressure transducer and internal thermocouple was similar to that assembly at the condenser end of the heat pipe. A stainless steel vacuum valve was welded to the pressure transducer end of the brass cylinder, with the brass cylinder properly ported internally, to fill the heat pipe with the working fluid and non-condensible gas as well as to evacuate the heat pipe prior to filling.

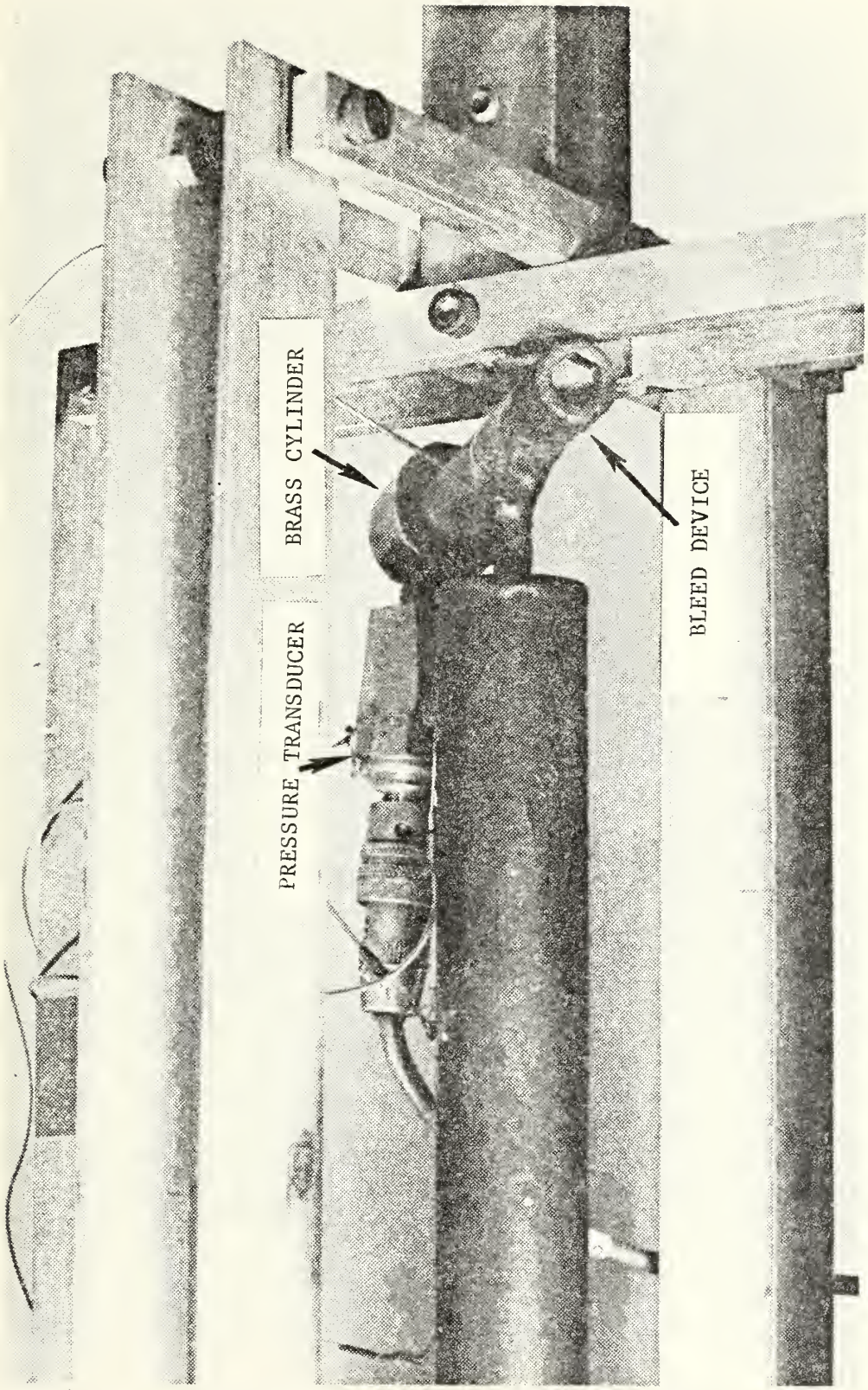

Photograph of Condenser End of Heat Pipe

Figure 3

The evaporator section was heated by passing a direct current through a 0.32-centimeter wide Nichrome ribbon, measuring 3.83 meters in length, wrapped around the heat pipe circumference. Both the heat pipe exterior and Nichrome ribbon were painted with high temperature heat-resistant paint prior to wrapping. This painting electrically insulated the Nichrome ribbon from the heat pipe. To minimize heat losses, four layers of 0.32-centimeter thick Johns Manville Min-K insulation were wrapped around the adiabatic and evaporator sections.

The supporting framework for the heat pipe was designed to allow rotation of the heat pipe from the horizontal (Figure 4) to vertical position (Figure 5) as well as to minimize conduction heat losses.

B. INSTRUMENTATION

Forty thermocouples were installed to measure accurately the required temperatures. Twenty-four thermocouples were tack welded externally at 5.1-centimeter intervals along the top of the condenser and adiabatic sections of the heat pipe. Additional thermocouples were tack welded at 90-degree angular intervals around the pipe at locations 27.9 and 73.7 centimeters from the condenser end to measure the circumferential temperature variation. To determine the insulation heat loss by measuring the temperature drop across a layer of insulation, two thermocouples were inserted between layers of insulation, and two thermocouples were placed atop the outside layer of insulation. As previously stated, a stainless steel sheathed thermocouple was welded into each end plate to measure the internal heat pipe temperature existing at the condenser and evaporator. These internal thermocouples, located slightly off the center of the endcaps, projected about 1.3

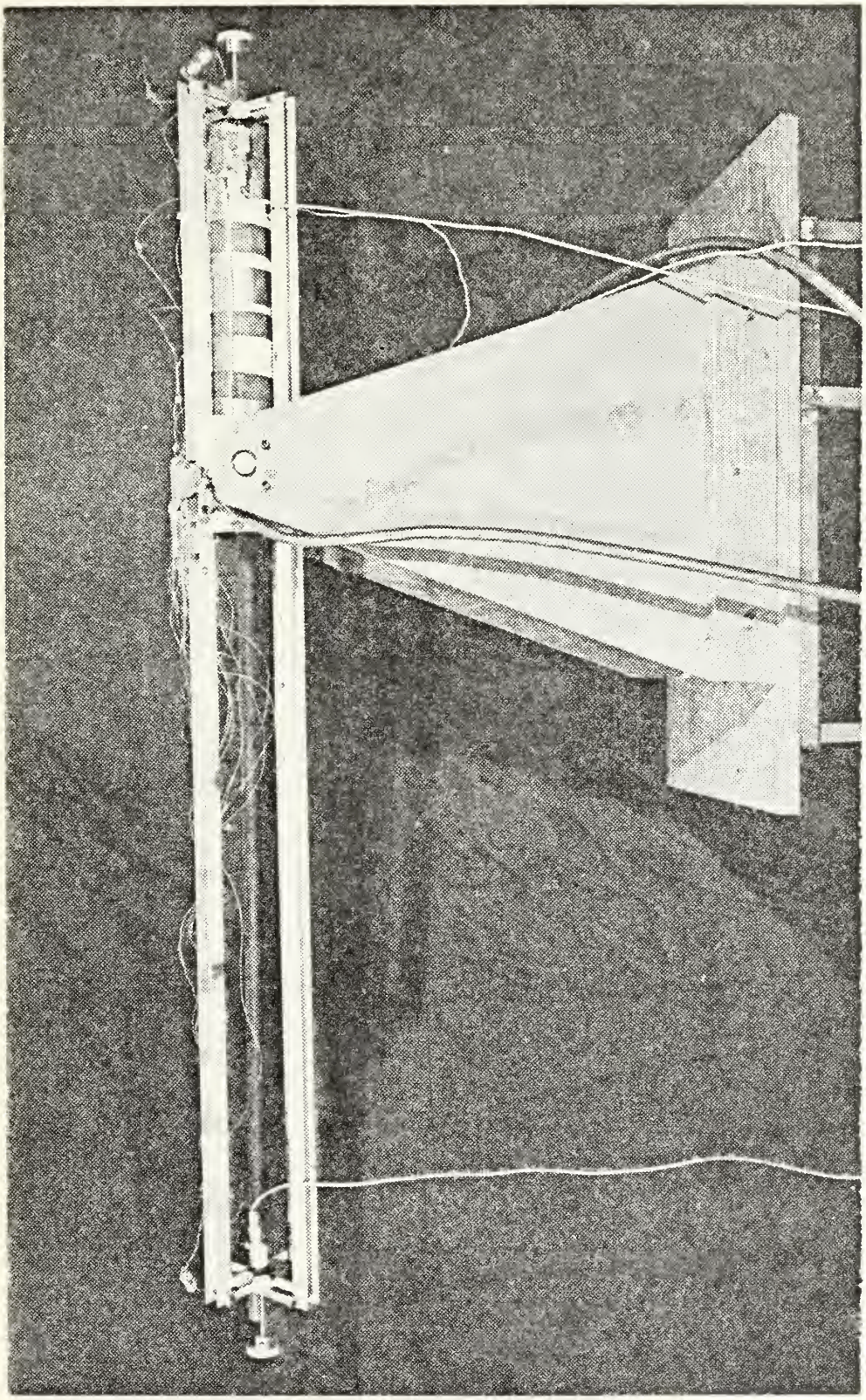

Photograph of Heat Pipe - Horizontal Position

Figure 4

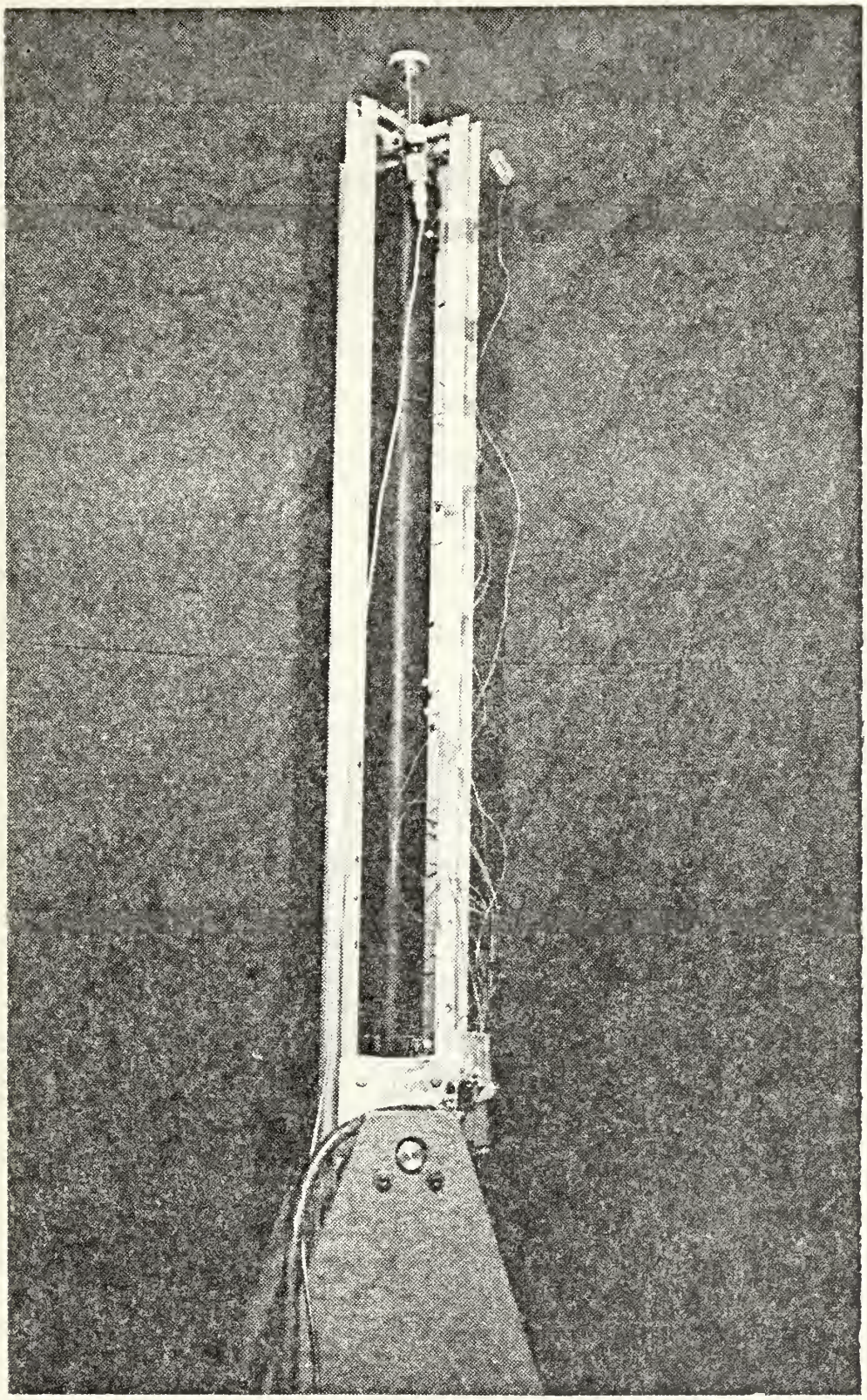

Photograph of Heat Pipe - Vertical Position

Figure 5

centimeters into the heat pipe interior from the end cap. Two thermocouples were used to measure the ambient room temperature existing near the condenser section.

The thermocouples were fabricated from 30 gage Teflon-coated copper and constantan wires, using a Dynatech thermocouple welder to make the end beads. Twenty of the thermocouple wire ends were soldered to the pins of the male half of an Amphenol connector. A 40-wire umbilical cable joined the female half of the Amphenol connector (which was attached to the heat pipe frame) to the Hewlett-Packard 2010C Data Acquisition System (Figure 6). The other 20 thermocouples were similarly connected to a second umbilical cable. The Amphenol connectors were covered with sponge rubber to minimize the effect of stray air currents passing through the connector which could cause erroneous temperature readings.

Pressure transducers were placed at both the condenser and evaporator ends of the heat pipe to measure the condenser and evaporator pressures. Celesco Model PLC Pressure Transducers, with a range of zero to 6.8 atmospheres, were used. The electrical output of the pressure transducers was recorded by the Hewlett-Packard 2010 Data Acquisition System.

To determine accurately the amount of power being supplied to the heat pipe, a known stable precision resistance was placed in series with the Nichrome ribbon heater. By measuring the voltage drop across this known resistor, the heater current could be calculated. Hence, the power being supplied to the heat pipe could be determined by knowing the heater current and measuring the voltage drop across the heater.

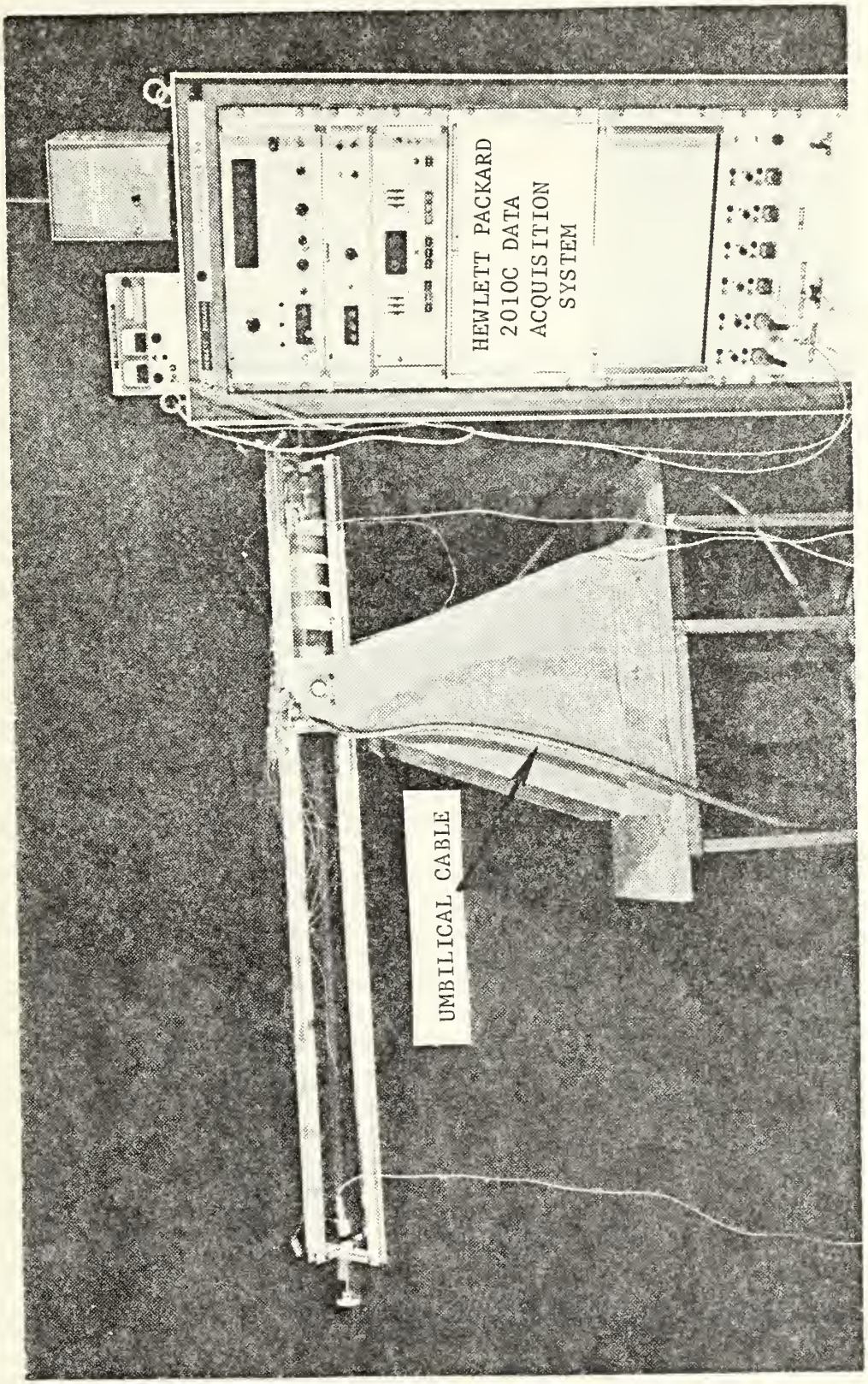

Photograph of the Entire Experimental Apparatus

Figure 6

The Hewlett-Packard 2010C Data Acquisition System digitally recorded all output voltages of the thermocouples and pressure transducers. This system also measured the voltage drops across the heater and the known resistor.

C. LIQUID CRYSTAL APPLICATION

Cholesteric liquid crystals were used in this experiment to show qualitatively the orientation of the vapor-gas interface relative to the heat pipe axis. As the liquid crystal is heated through a known range of temperature, it will exhibit progressively all colors of the spectrum, from red to violet. This phenomenon is both reversible and repeatable. The drastic temperature change across the vapor-gas interface of the variable conductance heat pipe provides the temperature range necessary to observe the color change of the liquid crystals.

The width of the temperature range and its location on the temperature scale can be controlled by choosing the proper cholesteric esters and formulating them in the correct proportions. National Cash Register Company has developed a process which encapsulates the liquid crystals in a polyvinyl alcohol. This encapsulation significantly extends the useful life and markedly reduces the color variation of the liquid crystals due to viewing angle. Also, encapsulated crystals which activate at different temperatures can be mixed without altering the color response of each individual liquid crystal, although mixing does decrease the brilliance of each liquid crystal color. Properties of these liquid crystals and several temperature-sensing applications are well described in Ref. [12].

Three different liquid crystals were chosen so that they would activate at a temperature between that of the condensing working fluid

and that of the non-condensible gas. R-53, R-45, and S-40 encapsulated liquid crystals, in a slurry form, were selected. The "R" indicates that the color change occurs uniformly in about a 3°C temperature range. The number denotes the activation temperature of the red color change. For example, the red color change for R-53 occurs at 53°C. The "S" indicates the liquid crystal changes from red to violet in about a 1.1°C temperature range.

Since the liquid crystals are transparent, the entire condenser section was spray painted with flat black enamel which provided a suitable, dark non-reflective background to observe the liquid crystals. A mixture consisting of equal parts of the three different liquid crystals was diluted with an equal volume of distilled water. This enabled several thin coats to be uniformly applied to the heat pipe using an air brush to spray on the liquid crystals.

D. CALIBRATION

A 3-meter mercury manometer was used as a standard to calibrate the pressure transducers for pressures from atmospheric to about five atmospheres. For pressures from atmospheric to about 0.5 atmospheres, a 1.5-meter U-tube mercury manometer was used as the standard. A first order equation relating millivolts to absolute pressure, using a least squares fit, was derived for each transducer. The transducers were not calibrated at various temperatures, but only at room conditions. The maximum error yielded by either equation was 0.5 per cent.

A Rosemount Calibration System, having a platinum resistance thermometer, was used as the temperature standard to calibrate the thermocouples. To minimize the effect of temperature variations within the oil bath,

the thermocouples were put into two 20-thermocouple bundles, with each bundle being placed as close as possible to the platinum resistance thermometer. This calibration system has a $\pm$ 0.01°C accuracy. Data were taken between 21 and 121°C. As a result, the normal copper-constantan thermocouple tables could be used with an accuracy of $\pm$ 0.5°C.

IV. EXPERIMENTAL PROCEDURE

A. EXPERIMENTAL PREPARATION

To provide comparability with previous data taken by Naydan [Ref. 9] and Batts [Ref. 10] on a 5.1-centimeter heat pipe, methanol was used as the working fluid, and helium and krypton were used as the non-condensible gases in these heat pipe experiments. Data were also taken using Freon 113 as the working fluid and helium as the non-condensible gas. Since the difference in molecular weights between Freon 113 and helium is significantly greater than for methanol and helium, gravitational forces should have a greater effect on the Freon 113-helium interface than on the methanol-helium interface.

The amount of methanol necessary to operate successfully the heat pipe and the maximum power level for heat pipe operation had to be determined. Naydan and Batts experimentally determined that 170 ml was a sufficient amount of methanol for the 5.1-centimeter diameter heat pipe they were operating. Since this heat pipe was a 2.5-centimeter diameter pipe and its wick volume was one-half the wick volume of the 5.1-centimeter heat pipe, 85 ml of methanol was used initially to fill this heat pipe. This 85 ml of methanol did prove to be sufficient to prevent the complete evaporation of the methanol that would result in dryout of the wick and subsequent heat pipe failure. After much experimentation, it was determined that 50 watts of nominal input power was the upper power limit.

To add the methanol to the heat pipe, a short length of vacuum tubing was connected to the fill valve of the heat pipe and a graduated

glass bottle containing the 85 ml of methanol (Figure 7). The glass bottle was inverted, and the methanol was allowed to displace the air entrapped in the fill valve and rubber tubing. The fill valve was opened, and the methanol entered the heat pipe since the pipe interior was under a vacuum. (The heat pipe had been evacuated previously using a vacuum pump, and the fill valve was then closed to maintain this vacuum.) During the filling operation, the heat pipe was in the horizontal position with no power being supplied.

To bleed the air introduced into the heat pipe during the filling operation, 75 watts of power were applied to the heat pipe in the vertical position (condenser end up) to raise the internal pipe pressure above atmospheric. The bleed device was then opened to vent the air which had accumulated in the condenser end of the heat pipe. Several vents were required to bleed successfully virtually all of the air. It was estimated that about three to five milliliters of methanol excaped during each vent.

B. METHANOL CONVENTIONAL HEAT PIPE EXPERIMENTATION

Upon the successful conclusion of the venting procedure, the heat pipe was operated in the conventional mode, in both the horizontal and vertical positions. Power was varied in 15-watt increments from 20 to 50 watts and then decreased to 20 watts to ensure data repeatability, in both heat pipe positions. The power levels were calculated from the measurement of the voltage drop across the heater and the known resistor. The power lost from the evaporator and adiabatic sections due to insulation losses was calculated from the temperature drops across the insulation. The net power absorbed by the heat pipe was assumed to be the calculated power produced in the heater minus the insulation losses. See Appendix A for sample calculations.

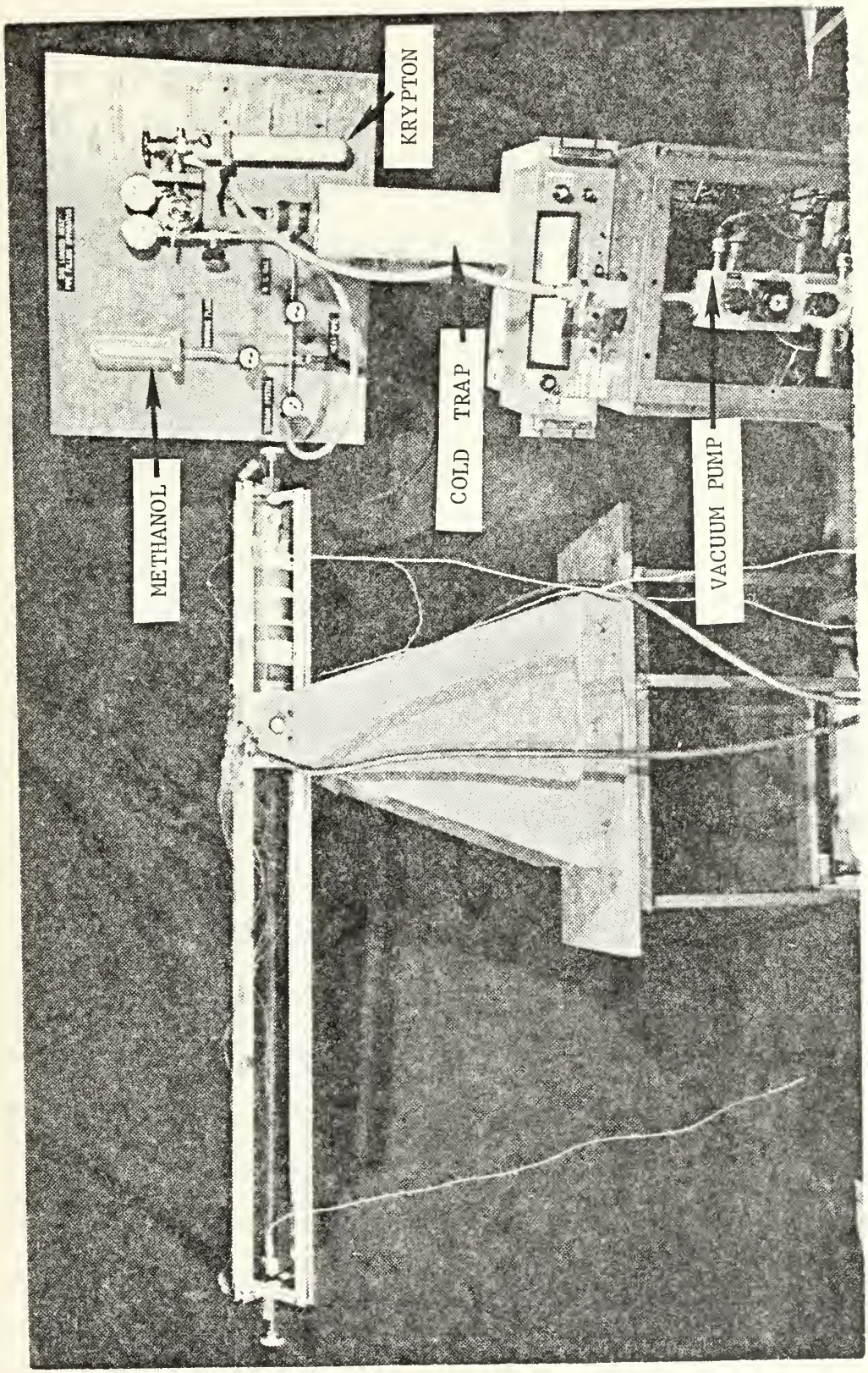

Photograph of Fill Assembly and Vacuum Pump

Figure 7

The following criterion was established to ensure that steady state conditions had approximately been reached after a power change to the heater. When the temperature difference between the evaporator end and ambient conditions showed a change of less than 0.5°C in a 15-minute period, approximate steady state conditions had been attained, and data could then be recorded. All data were taken at least three and one-half hours after a heater power change. This steady state criterion was used for all subsequent heat pipe data, whether the heat pipe was operating in the conventional or variable conductance mode.

C. METHANOL-KRYPTON VARIABLE CONDUCTANCE HEAT PIPE EXPERIMENTATION

After all the data had been taken for the methanol heat pipe operating in the conventional mode, the non-condensible gas krypton was introduced into the heat pipe, thereby making it a variable conductance device. The following procedure was used to load the krypton. The fill rig system (Figure 7) was evacuated to a pressure of about 1.31×10^{-7} atmospheres, purged with a small amount of krypton, and re-evacuated to the aforementioned pressure. A cold trap was used to condense the purging krypton in order to prevent krypton contamination of the vacuum pump. With the heat pipe operating at 35 watts of power in the horizontal position, the fill system was pressurized with krypton up to the fill valve on the heat pipe, and the fill valve was slowly opened. The fill valve was secured when the pressure in the heat pipe increased a predetermined amount — 0.90 atmospheres in this instance.

To determine the exact amount of krypton loaded into the heat pipe, electrical power was secured to the pipe, and the device was allowed to

reach steady state at ambient conditions. The internal heat pipe pressure measured by the pressure transducers was recorded. The average value of the evaporator and condenser temperatures, measured by the two internal thermocouples, was used as the saturation temperature of the methanol vapor to enter the methanol saturated vapor table. The extracted tabular value was the partial pressure of methanol at that particular saturation temperature. The partial pressure of krypton was found by subtracting the partial pressure of methanol from the total pressure. Knowing the heat pipe volume, the internal temperature, and the partial pressure of krypton, the amount of krypton in the heat pipe was calculated. Appendix B shows sample calculations to determine the amount of non-condensible gas present in the heat pipe.

With the initial charge of krypton, heat pipe data were taken at the same power levels as in the conventional mode, in both the horizontal and vertical positions. After recording this data, the pipe was vented to remove about one-half of the krypton by reducing the pipe pressure an appropriate amount. However, it was determined that the krypton load was actually about one-third of its initial value. When the necessary data had been recorded, the heat pipe was again vented to make the third krypton load about one-quarter of the original krypton charge. However, this effort was unsuccessful since this last krypton load was about .003 of the initial krypton load.

Both pressure transducers yielded erroneous readings while taking data for this third krypton load. These pressure transducer malfunctions will be discussed in the "Experimental Results" section.

With the aid of an outside protractor template made to match the outer pipe diameter, the angular position (from 0° to 180°, where the

0°-point was the top of the heat pipe in the horizontal position) of each liquid crystal isotherm was measured at 5.1-centimeter intervals along the condenser section. All measurements were made at the beginning of the green color change.

D. METHANOL-HELIUM VARIABLE CONDUCTANCE HEAT PIPE EXPERIMENTATION

The methanol-krypton mixture was removed completely from the heat pipe using a vacuum pump and cold trap. The cold trap condensed the methanol-krypton mixture which would have otherwise contaminated the vacuum pump. The pressure transducers were recalibrated; and a new first order equation, relating absolute pressure to millivolts, was derived for each transducer. The heat pipe was filled with about 85 ml of methanol and properly vented of air. Sufficient helium was added to raise the heat pipe pressure by about 2.1 atmospheres. After the necessary data were recorded, venting was adjusted to make the second and third helium loads roughly one-half and one-quarter, respectively, of the original helium load.

E. FREON 113 CONVENTIONAL HEAT PIPE EXPERIMENTATION

The methanol-helium mixture was evacuated from the heat pipe using a vacuum pump and cold trap. The heat pipe was filled with about 120 ml of Freon 113 (distilled once) and vented of air. The necessary data were recorded. The evaporator pressure transducer yielded incorrect readings when these data were taken. Since the condenser pressure transducer was operating properly, it was decided to continue the experiment without recalibrating the evaporator transducer.

F. FREON 113-HELIUM VARIABLE CONDUCTANCE HEAT PIPE EXPERIMENTATION

Sufficient helium was added to raise the heat pipe pressure by about 2.1 atmospheres. After the requisite data were recorded, venting was

adjusted to make the second helium load about one-half of the original helium charge. However, the second helium charge was actually .033 of the initial helium load. Enough helium was introduced to make the third helium load roughly one-half of the initial helium load (Table I). The procedure used to calculate the helium present for each load was similar to that method used for the methanol-helium calculations (Appendix B), except that the Freon 113 saturated vapor table was used to determine the appropriate Freon 113 partial pressure.

TABLE I

HEAT PIPE LOADING

RUN	GAS	METHANOL LOAD (ml)	GAS LOAD (kg)	GAS PARTIAL PRESSURE AT AMBIENT TEMP. (atm.)
1	None	85	-	-
2	KRYPTON	85	1.59×10^{-3}	0.79
3	KRYPTON	85	6.17×10^{-4}	0.30
4	KRYPTON	85	5.49×10^{-6}	0.003
5	HELIUM	87	1.24×10^{-4}	1.27
6	HELIUM	87	6.17×10^{-5}	0.64
7	HELIUM	87	3.05×10^{-5}	0.31
		FREON 113 LOAD (ml)		
8	None	120	-	-
9	HELIUM	120	1.42×10^{-4}	1.47
10	HELIUM	120	4.72×10^{-6}	0.05
11	HELIUM	120	8.26×10^{-5}	0.85

V. EXPERIMENTAL RESULTS

A. GENERAL CONSIDERATIONS

Appendix C summarizes the important heat pipe parameters for each data run. In one instance, an asterisk appears beside the "Evaporator Temperature" entry. This indicates that the heat pipe was apparently operating at or near burnout conditions. The specific cause for this condition was not determined.

As previously mentioned, when the last set of methanol-krypton data was taken, the two pressure transducers suddenly yielded erroneous readings. Both transducers were then recalibrated, and a new first order equation, relating millivolts to absolute pressure, was derived for each transducer. The only difference between the original and new equations for each transducer was a change in the y-intercept value. Hence, the zero point of each transducer had shifted. Since both transducers had experienced a moderately wide range of temperatures during the experiment, it was considered that this temperature variation had caused these pressure transducer malfunctions. The evaporator pressure transducer operated improperly when the conventional Freon 113 data were taken. However, it was deemed not critical to recalibrate this transucer since the condenser transducer was operating normally.

B. CONVENTIONAL HEAT PIPE RESULTS

Figure 8 shows the temperatures along the condenser at one power setting for the methanol only heat pipe, and Figure 9 indicates the same parameters for the Freon 113 only pipe. These figures have

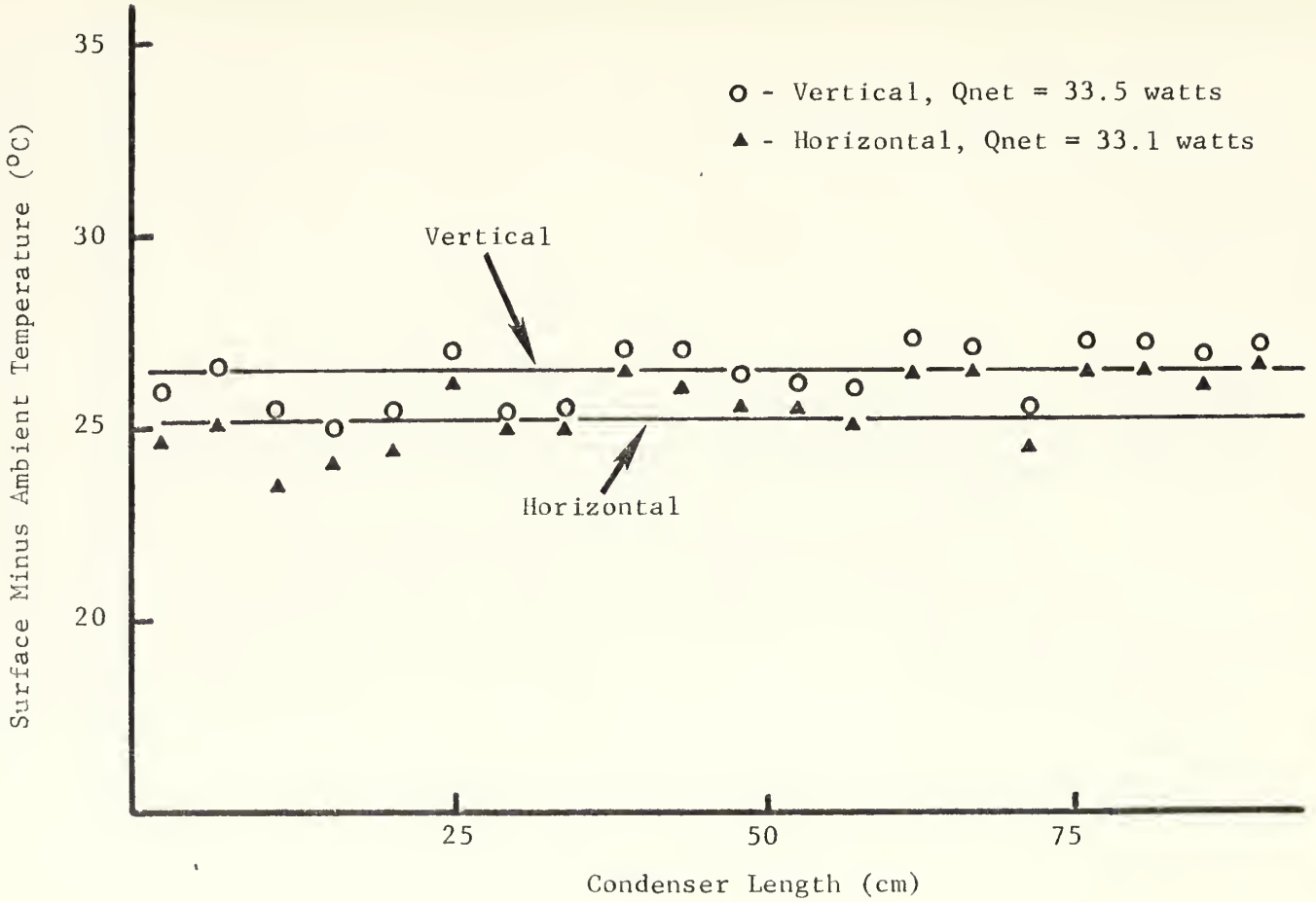

Surface Minus Ambient Temperature vs. Condenser Length -
Horizontal and Vertical - Methanol Only

Figure 8

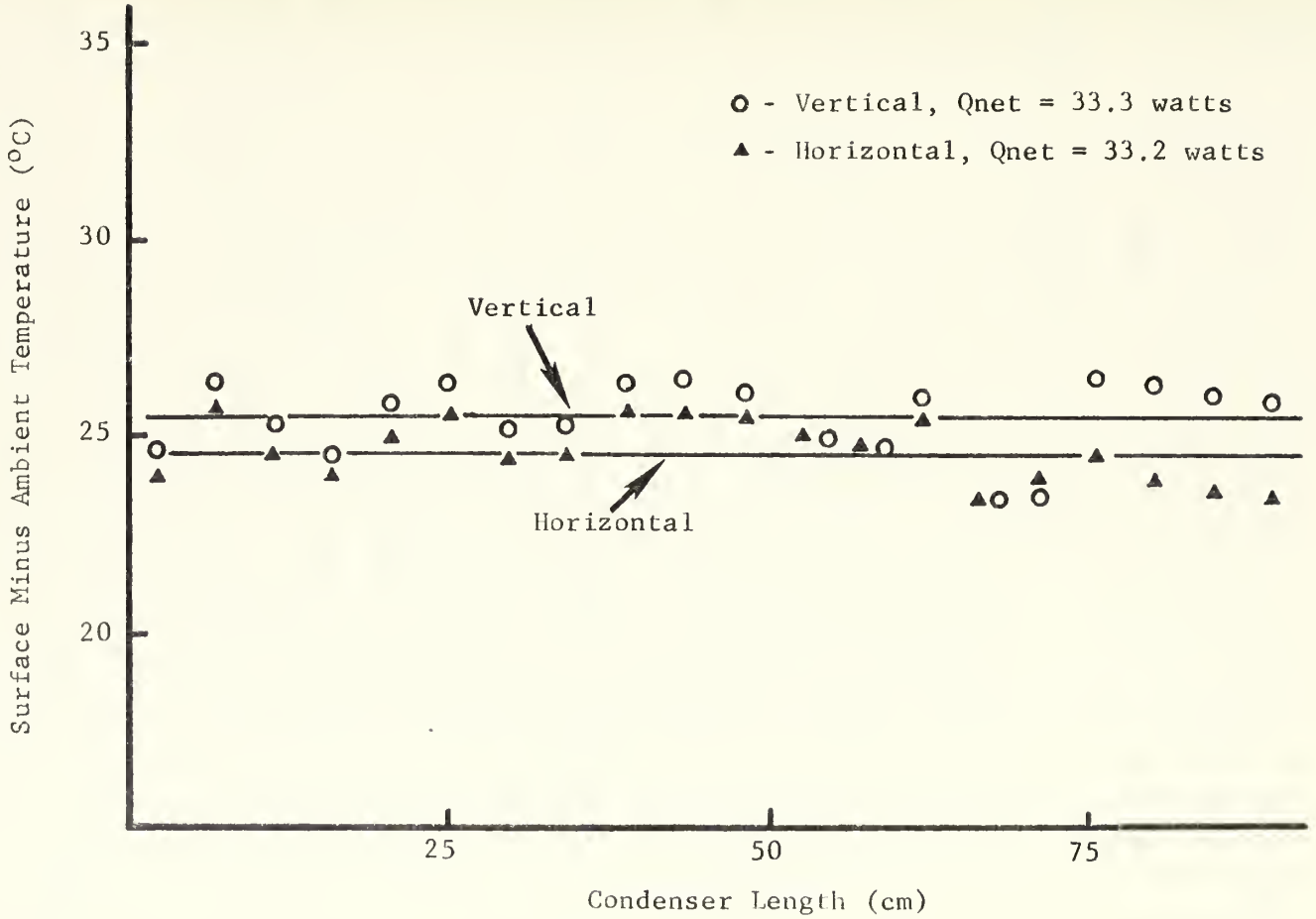

Surface Minus Ambient Temperature vs. Condenser Length -
Horizontal and Vertical - Freon 113 Only

Figure 9

"Surface Temperature Minus Ambient Temperature" as the ordinate axis. This axis selection eliminates the dependence of heat pipe performance parameters on a change in ambient temperature. Hence, comparisons can be made between various data runs even though the ambient temperature was different for each run.

These conventional heat pipes should operate at essentially isothermal conditions. Figures 8 and 9 support this premise, even though there are small temperature variations along the condenser length.

C. METHANOL-KRYPTON HEAT PIPE RESULTS

Figures 10 through 15 are the isotherms plotted from the liquid crystal data. As previously stated, these data were obtained by using an outside protractor to measure the angular position of the liquid crystal isotherms appearing on the heat pipe's circumference. These graphs represent one-half of the circular heat pipe circumference "rolled out" to a plane. Although there is some distortion in such a two-dimensional representation, the relevant information concerning the direction of the temperature gradients is retained. Figures 16 and 17 are the liquid crystal isotherms obtained by Batts [Ref. 10] for the 5.1-centimeter diameter heat pipe, using the methanol-krypton combination for one krypton load. Batts' figures favorably compare qualitatively with Figures 10 and 13. Batts also has photographs of the liquid crystal color bands for the methanol-krypton heat pipe; his photographs reflect the same general orientation of the liquid crystal isotherms that are presented in Figures 16 and 17. For comparable cases with the heat pipe in the horizontal position, the isotherms obtained by Batts will be closer to the horizontal in orientation than the isotherms resulting from this experiment.

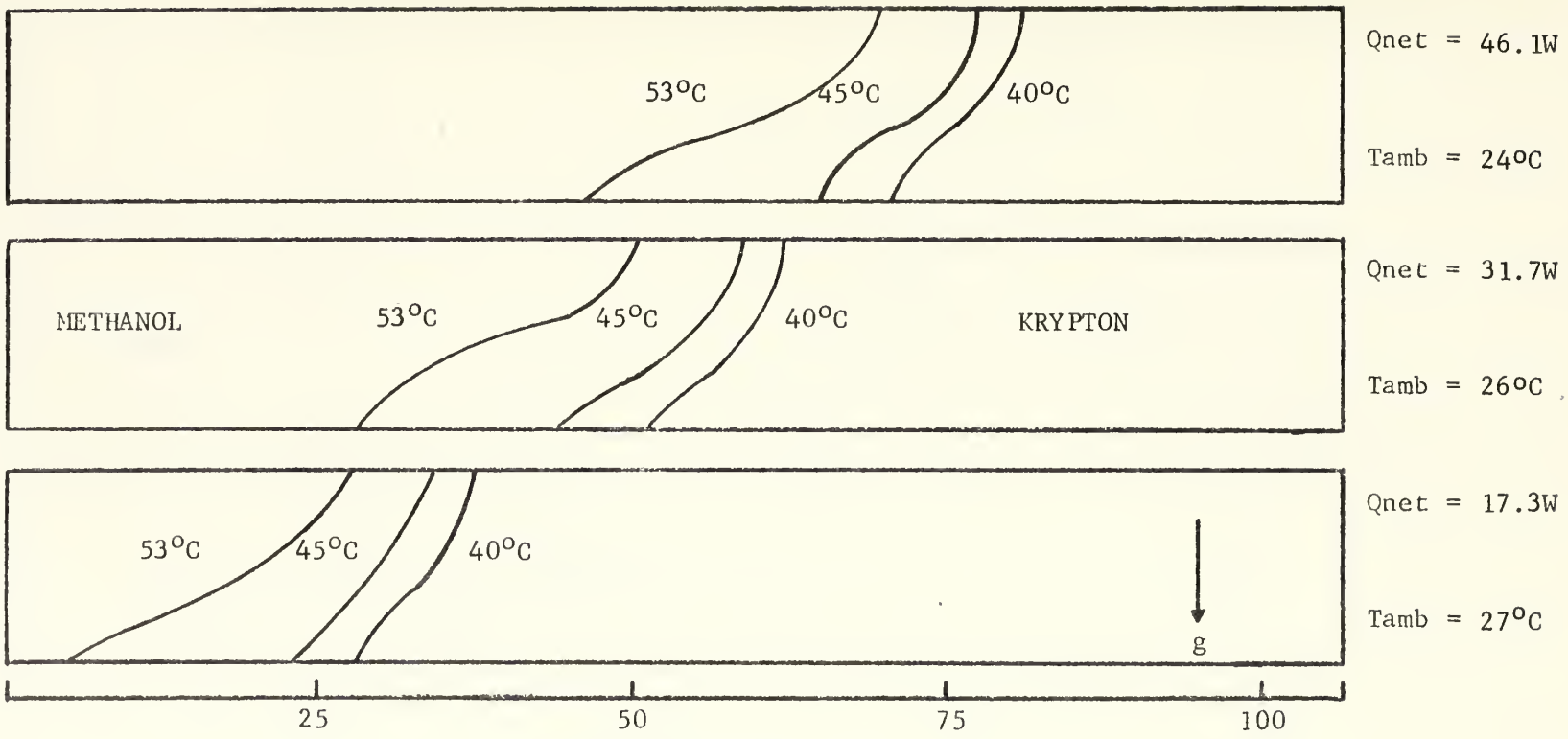

Liquid Crystal Isotherms - Horizontal - 1.59×10^{-3} kg Krypton

Figure 10

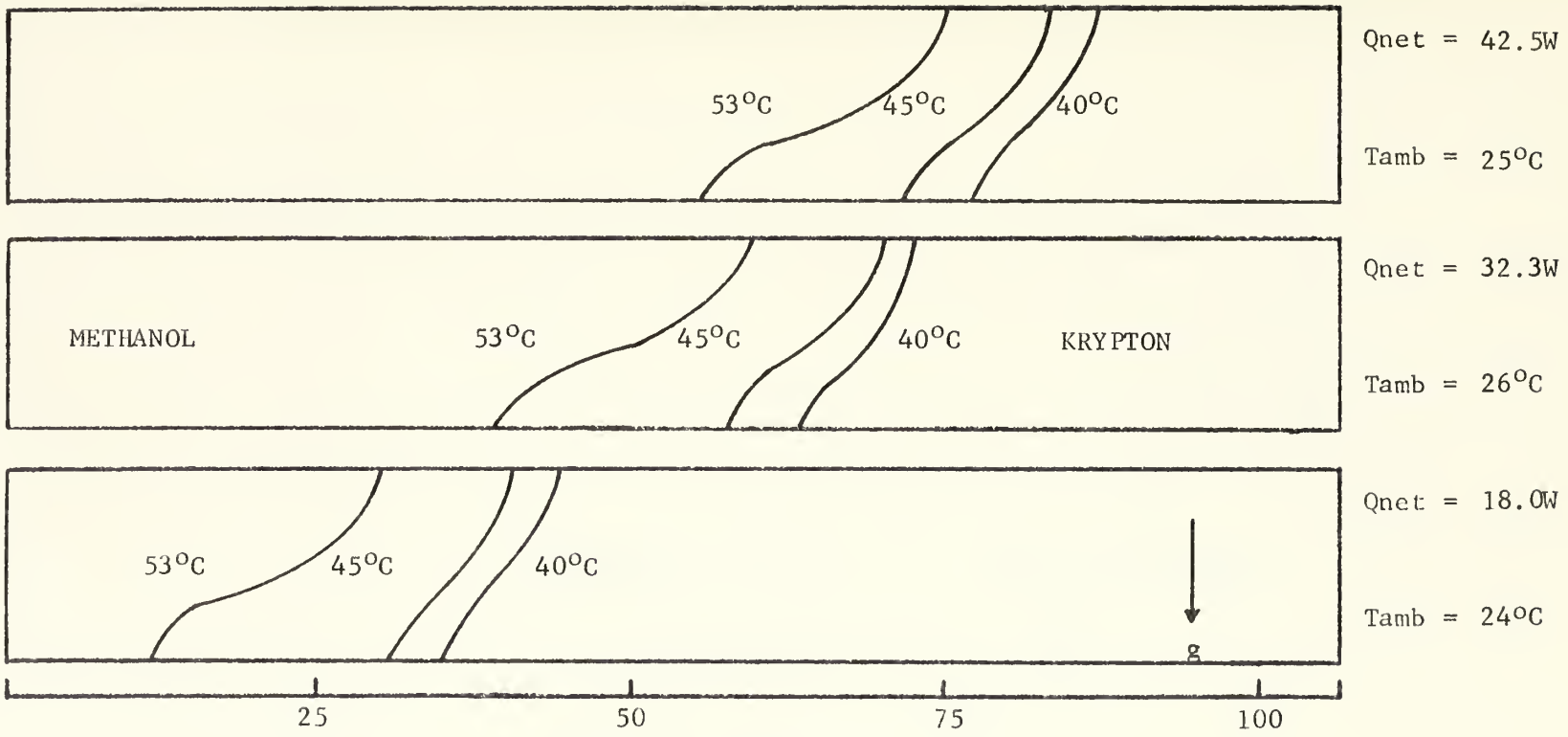

Liquid Crystal Isotherms - Horizontal - 6.17×10^{-4} kg Krypton

Figure 11

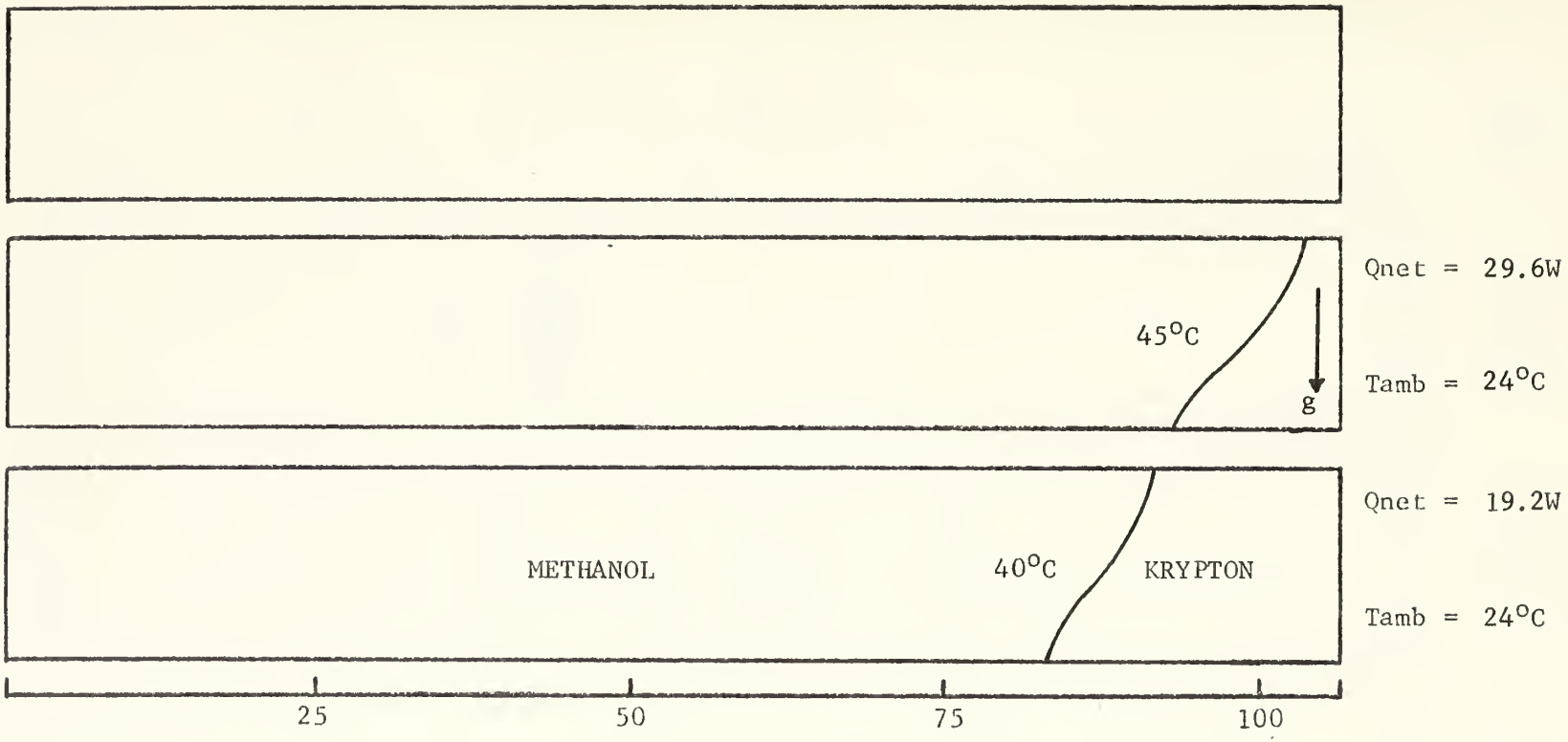

Liquid Crystal Isotherms - Horizontal - 5.49×10^{-6} kg Krypton

Figure 12

Qnet =	17.5W	31.7W	46.5W
Tamb =	27°C	25°C	25°C

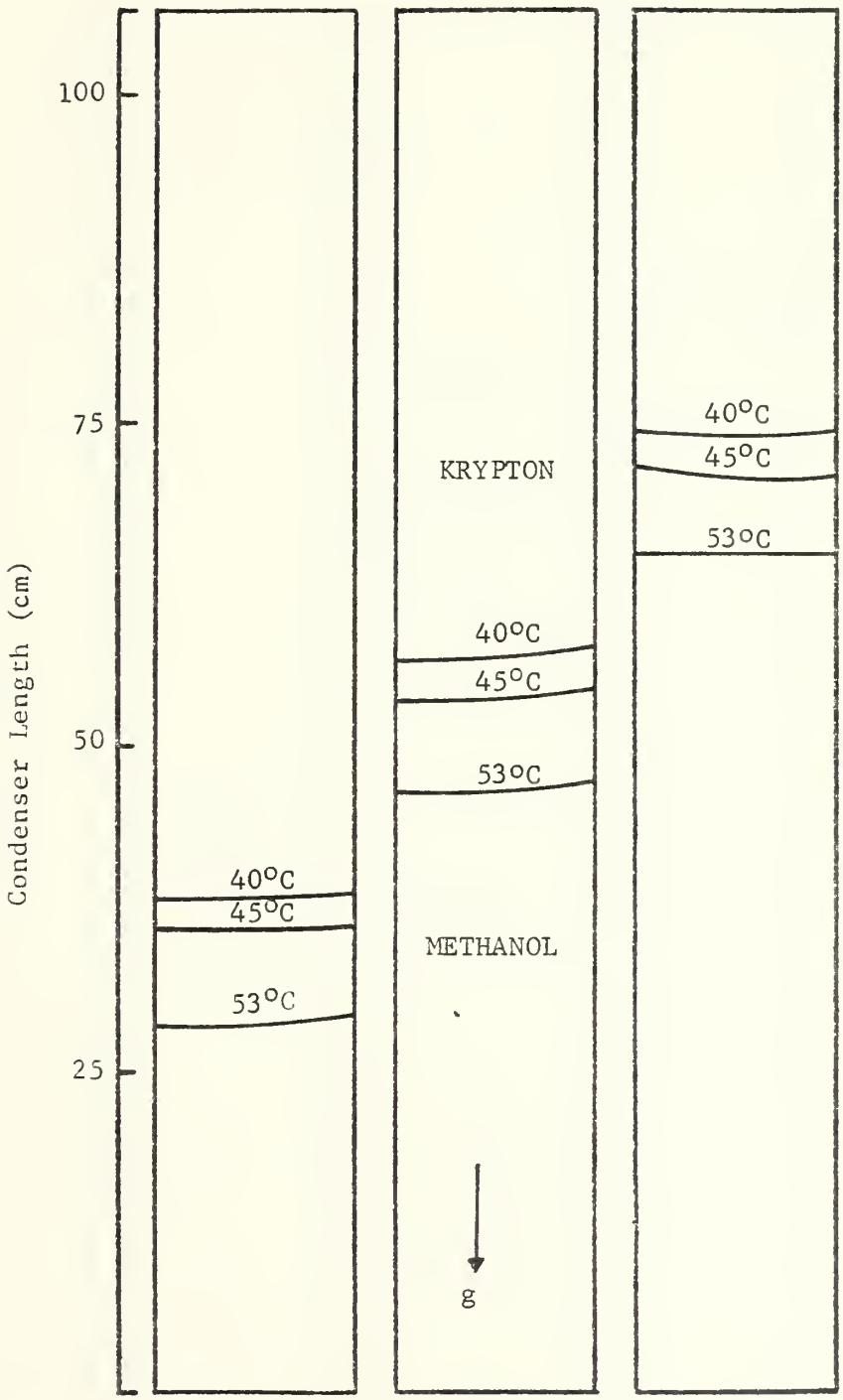

Liquid Crystal Isotherms - Vertical
1.59×10^{-3} kg Krypton

Figure 13

Qnet =	18.2W	32.5W	47.3W
Tamb =	24°C	25°C	27°C

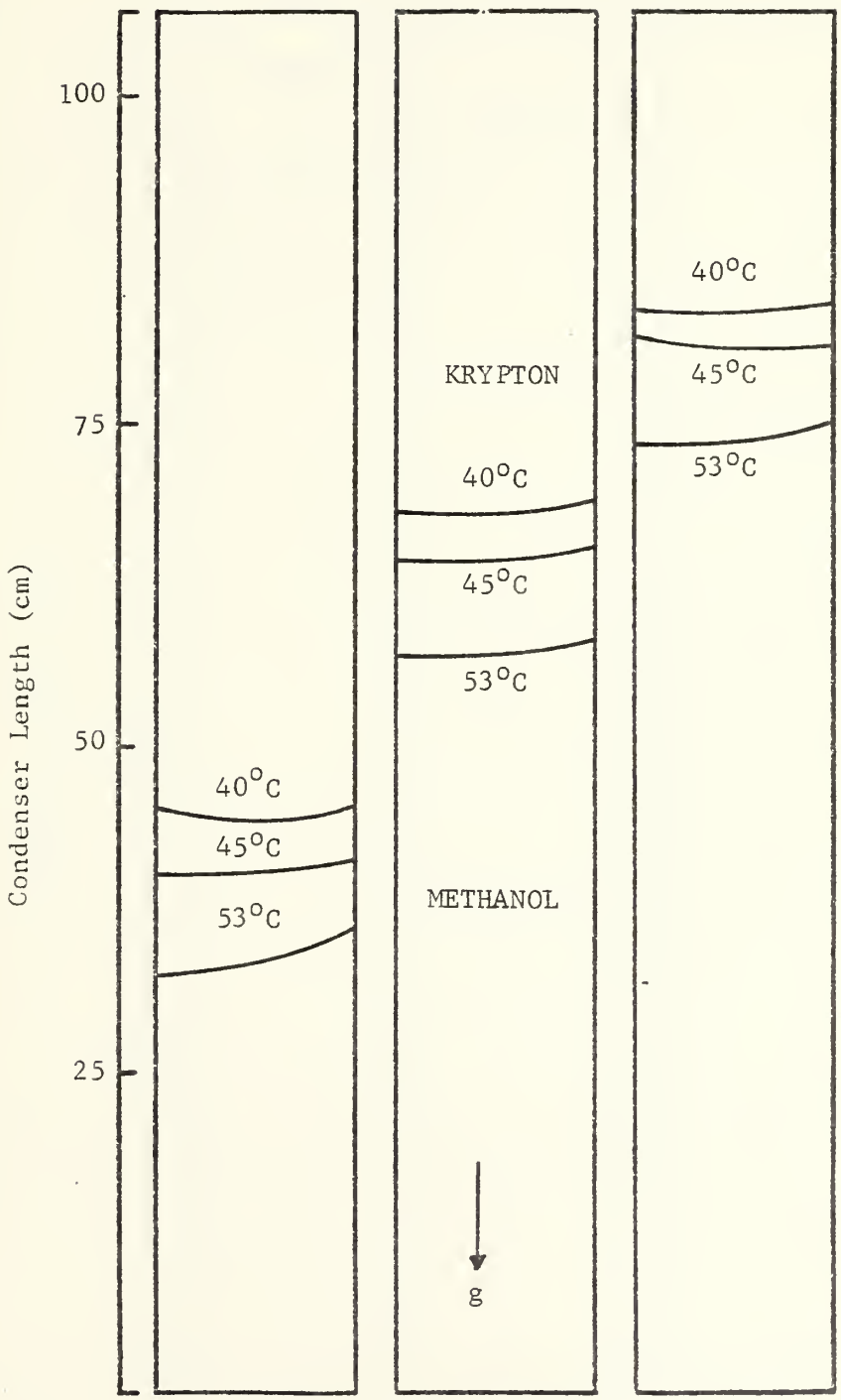

Liquid Crystal Isotherms - Vertical
6.17×10^{-4} kg Krypton

Figure 14

Qnet =	19.2W	33.4W
Tamb =	26°C	26°C

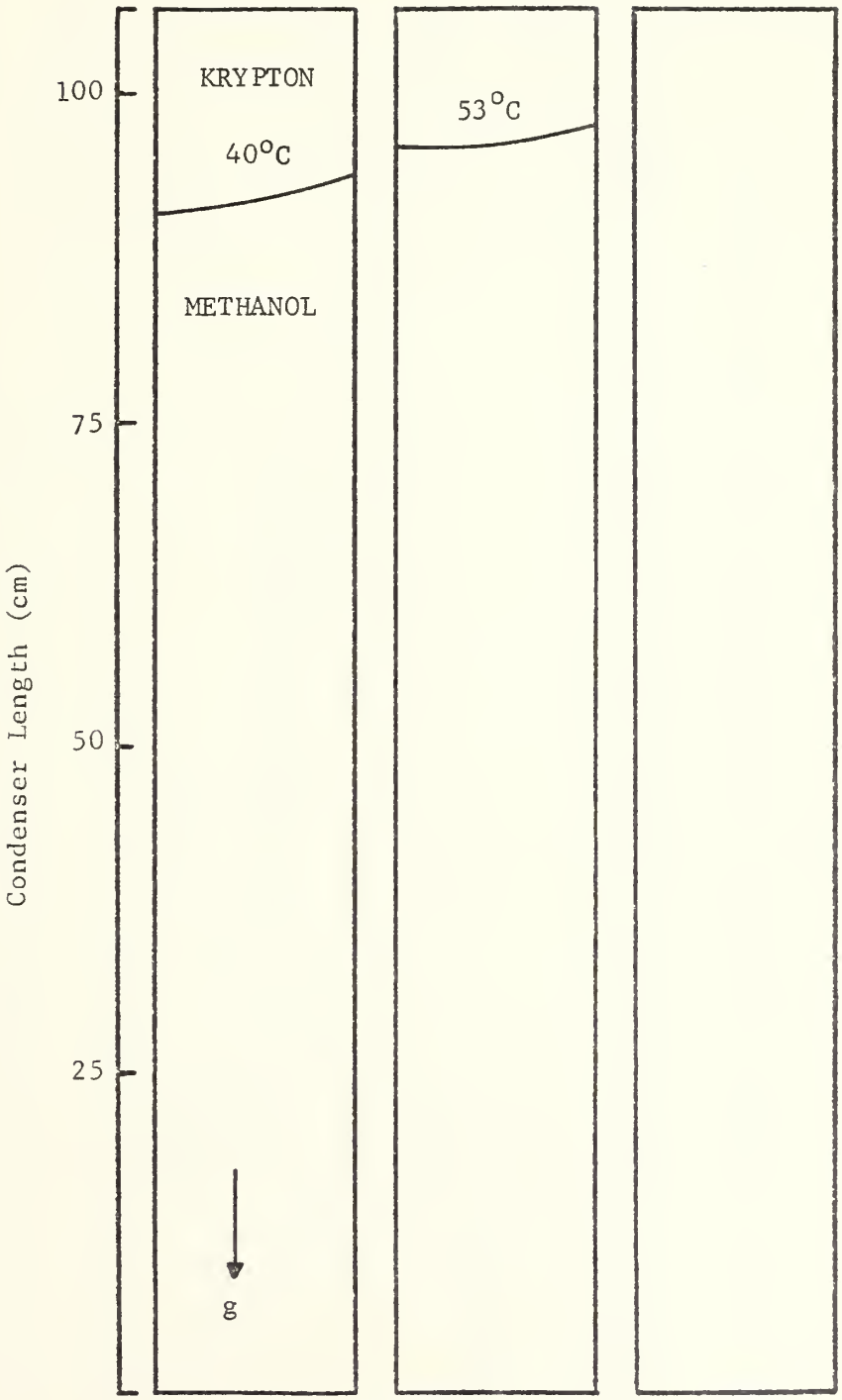

Liquid Crystal Isotherms - Vertical
5.49×10^{-6} kg Krypton

Figure 15

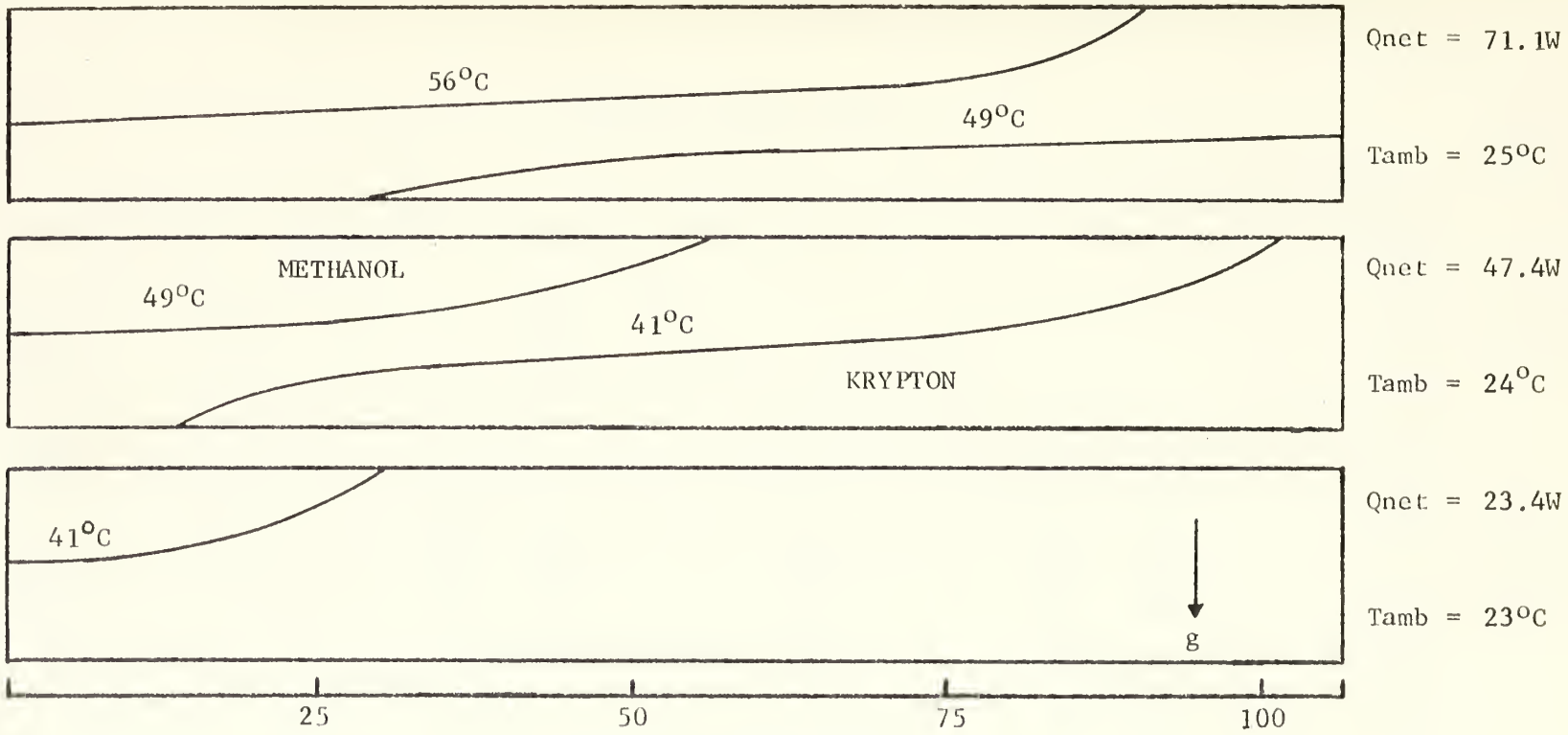

Liquid Crystal Isotherms - Horizontal - 2.75 x 10^{-3} kg Krypton - Batts' Results

Figure 16

Qnet =	22.9W	46.6W	70.2W
Tamb =	25°C	26°C	26°C

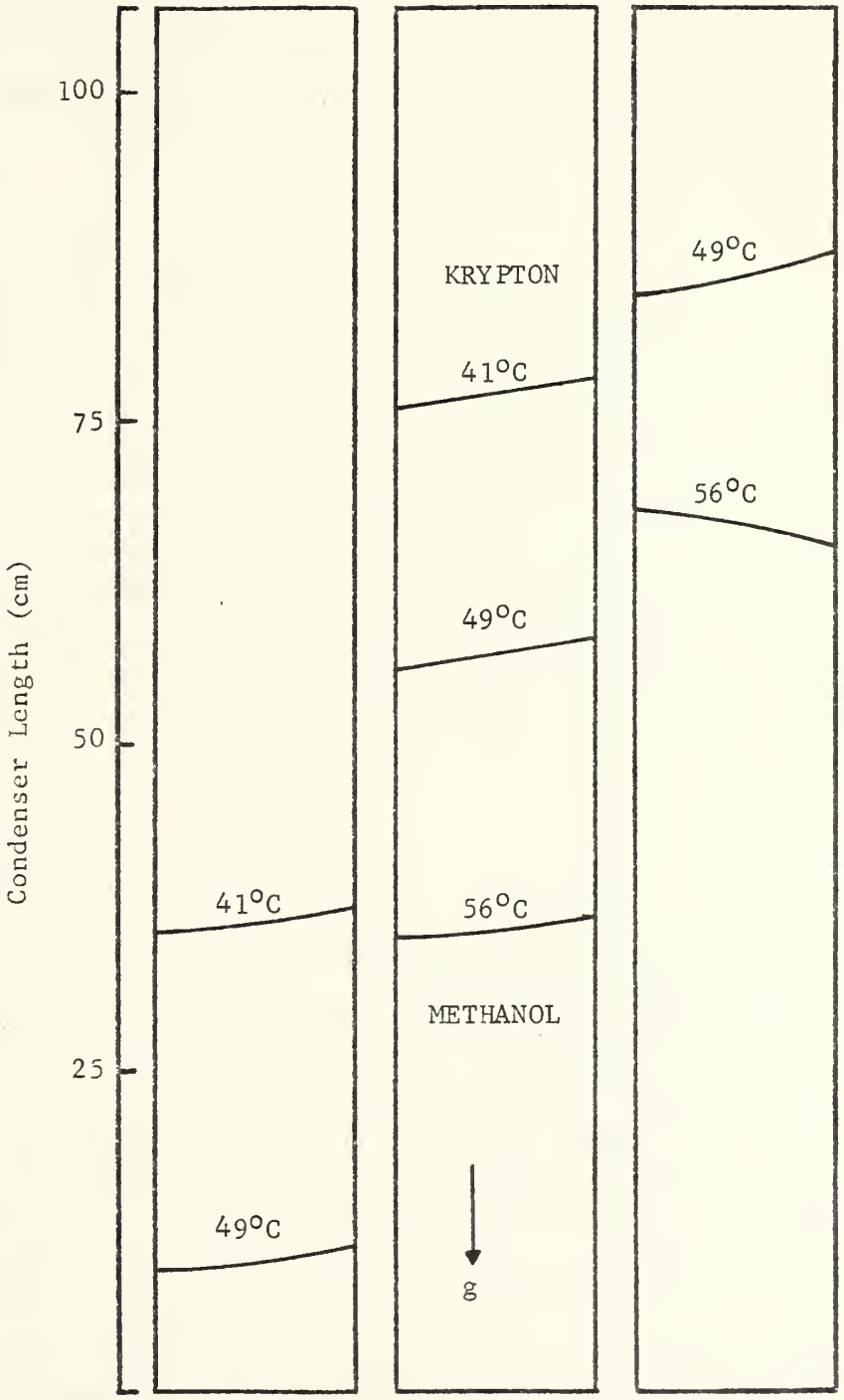

Liquid Crystal Isotherms - Vertical

2.75×10^{-3} kg Krypton - Batts' Results

Figure 17

D. METHANOL-HELIUM HEAT PIPE RESULTS

The liquid crystal isotherms for the methanol-helium heat pipe are Figures 18 through 23. These figures qualitatively confirm the results previously obtained by Batts, some of which are shown in Figures 24 and 25. Batts also has photographs of the liquid crystal isotherms for a methanol-helium heat pipe, which compare favorably with Figures 24 and 25.

E. FREON 113-HELIUM HEAT PIPE RESULTS

Figures 26 through 30 are the liquid crystal isotherms for the Freon 113-helium heat pipe. For the 4.72×10^{-6} kg load of helium, no liquid crystal isotherm measurements were taken since no definitive isotherms were observed. The liquid crystal isotherms were not symmetrical (with respect to the 0° and 180° reference points) for the heat pipe in the horizontal position. It is believed that this asymmetry was due to localized high conductance between the wick and heat pipe wall.

F. CONCLUSIONS

The orientation of the resulting liquid crystal isotherms for the methanol-helium, methanol-krypton, and Freon 113-helium heat pipes in the horizontal position clearly shows that the non-condensible gas did not form a plug at the condenser end of the pipe, as the flat front and diffuse front theories would predict. As these isotherms qualitatively reflect, there was a significant temperature gradient perpendicular to the heat pipe axis, in addition to the expected axial temperature gradient. Additionally, these isotherms show that there was a marked difference in the non-condensible gas concentration from

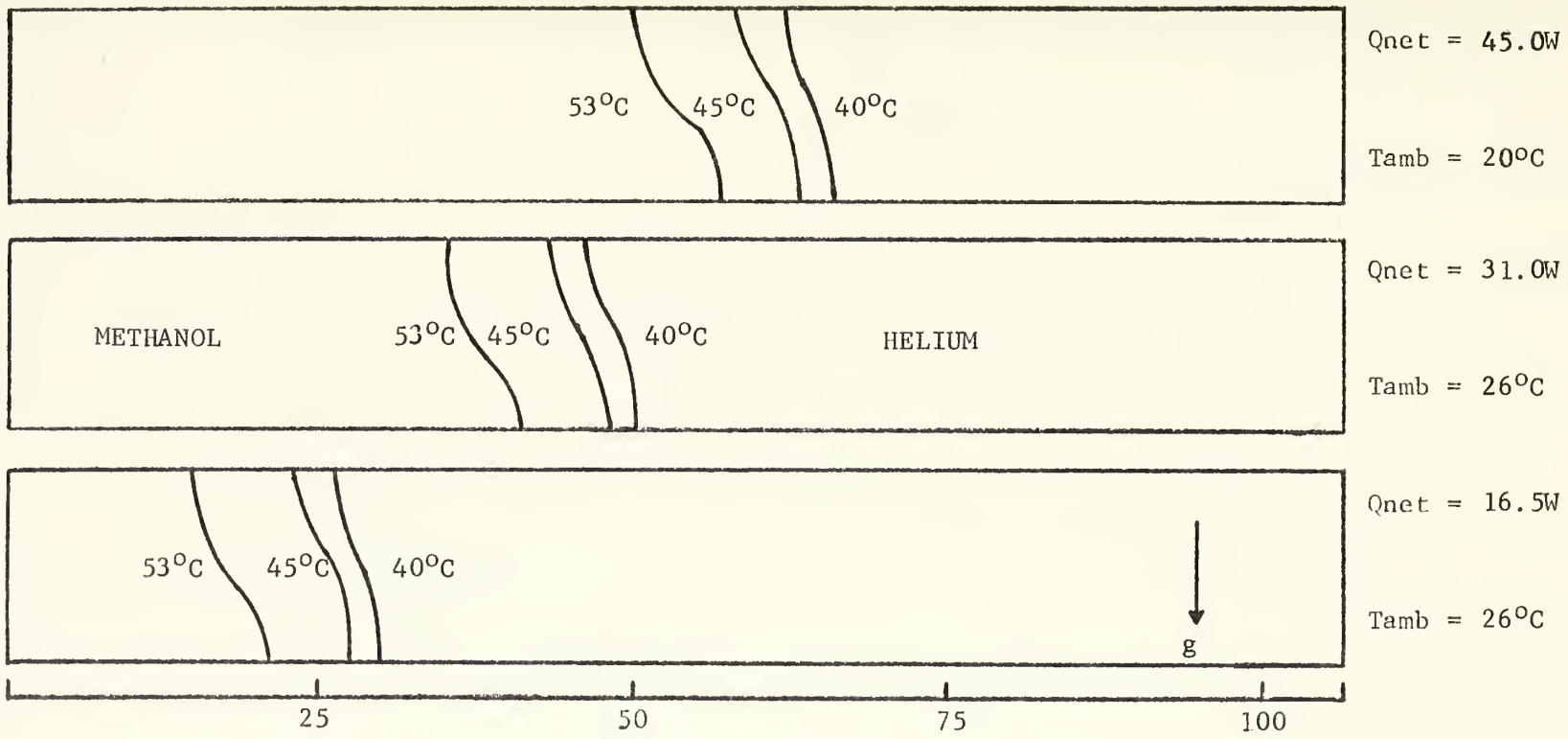

Liquid Crystal Isotherms - Horizontal - 1.24×10^{-4} kg Helium

Figure 18

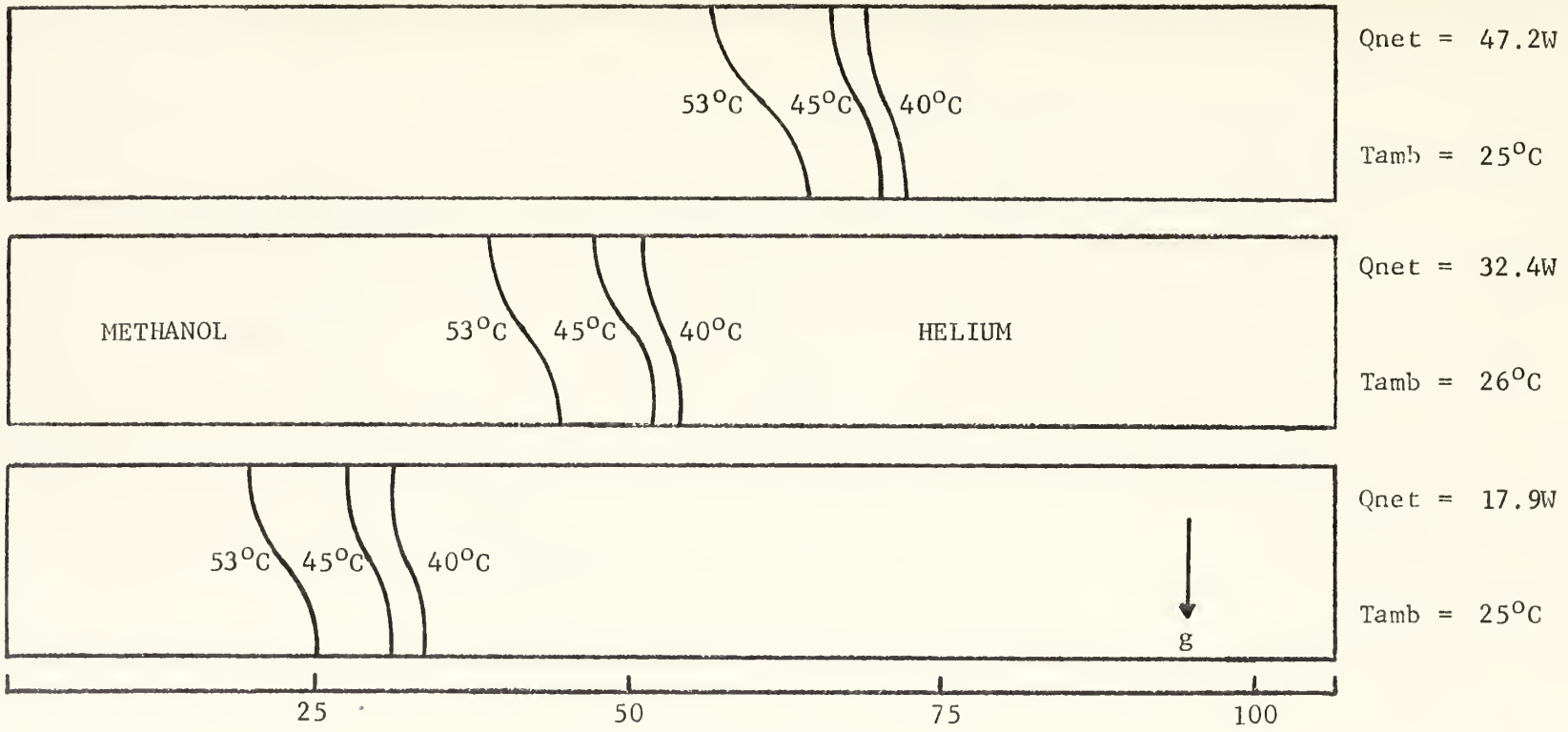

Liquid Crystal Isotherms - Horizontal - 6.17×10^{-5} kg Helium

Figure 19

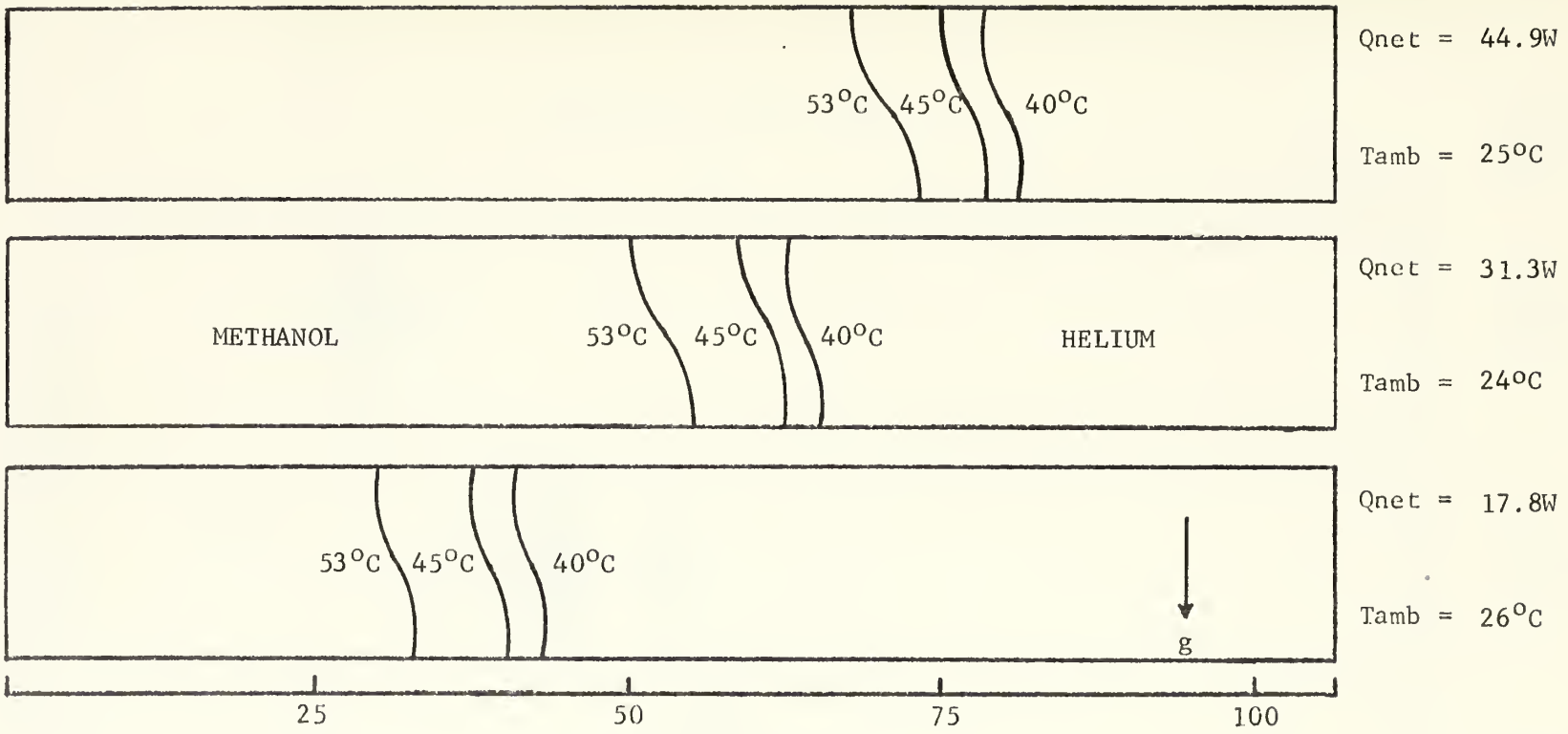

Liquid Crystal Isotherms - Horizontal - 3.05×10^{-5} kg Helium

Figure 20

Qnet =	16.9W	31.4W	45.9W
Tamb =	26°C	26°C	26°C

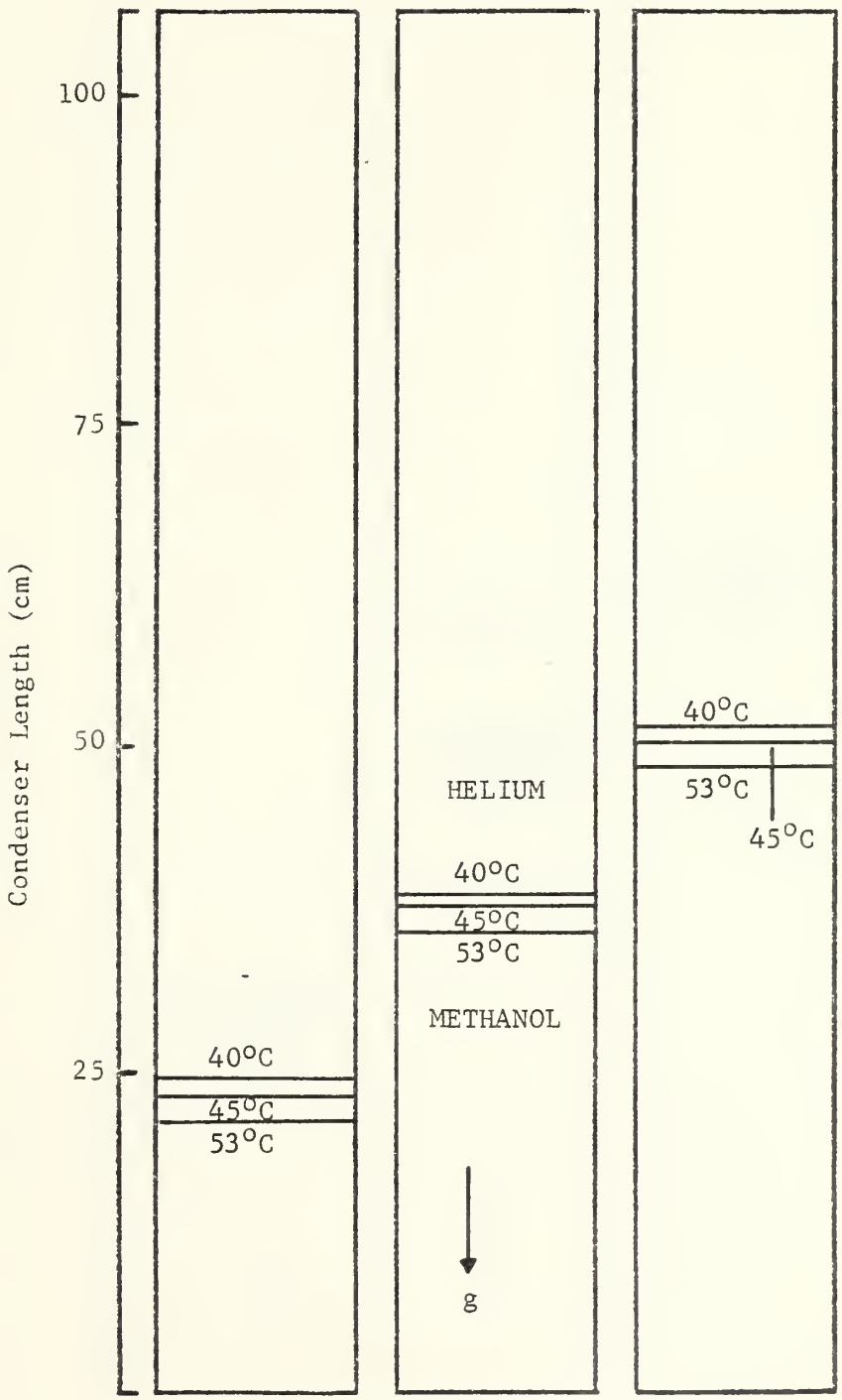

Liquid Crystal Isotherms - Vertical
1.24×10^{-4} kg Helium

Figure 21

Qnet =	18.2W	32.5W	47.0W
Tamb =	23°C	25°C	24°C

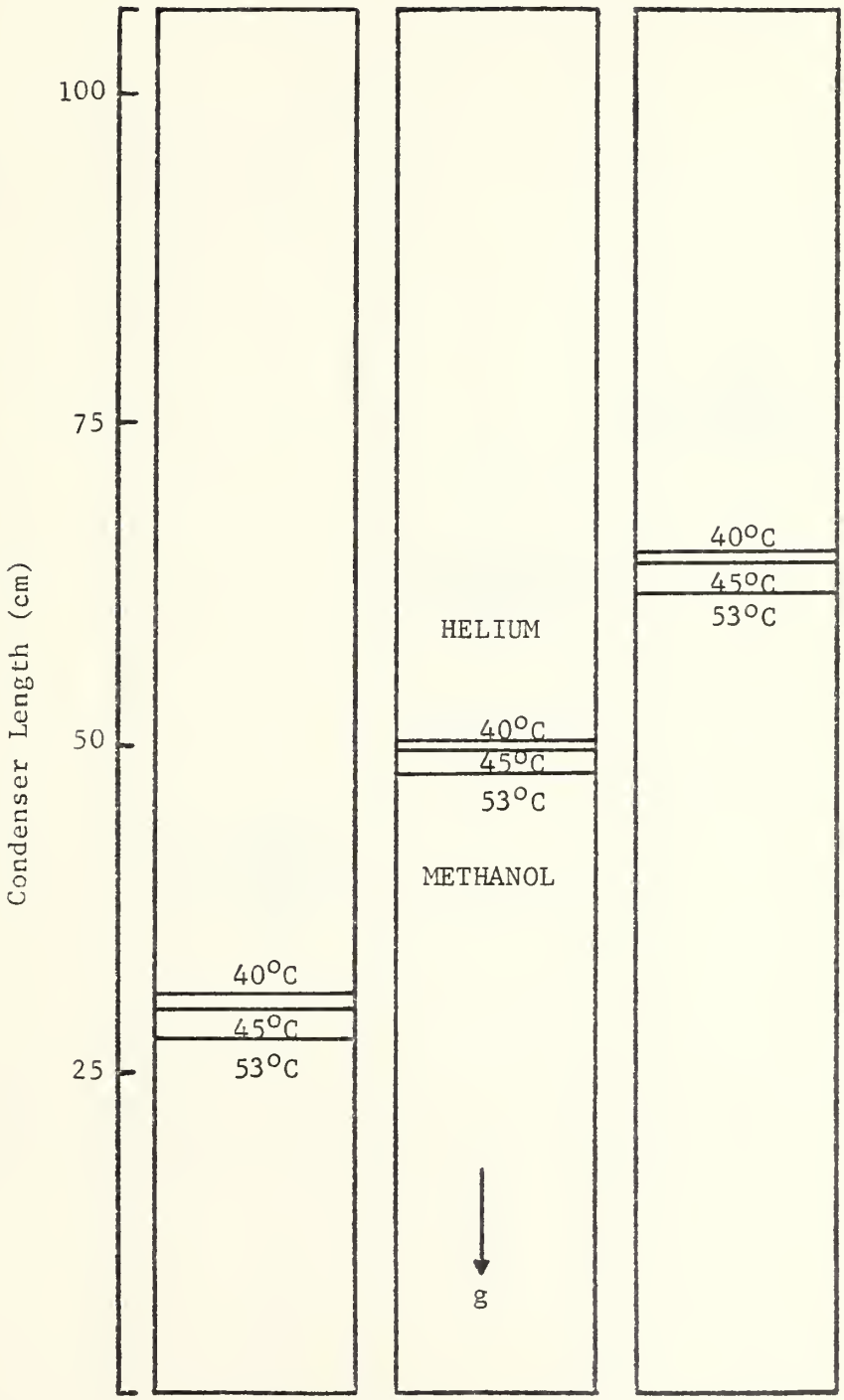

Liquid Crystal Isotherms - Vertical
6.17×10^{-5} kg Helium

Figure 22

Qnet =	18.5W	32.5W	47.3W
Tamb =	25°C	27°C	25°C

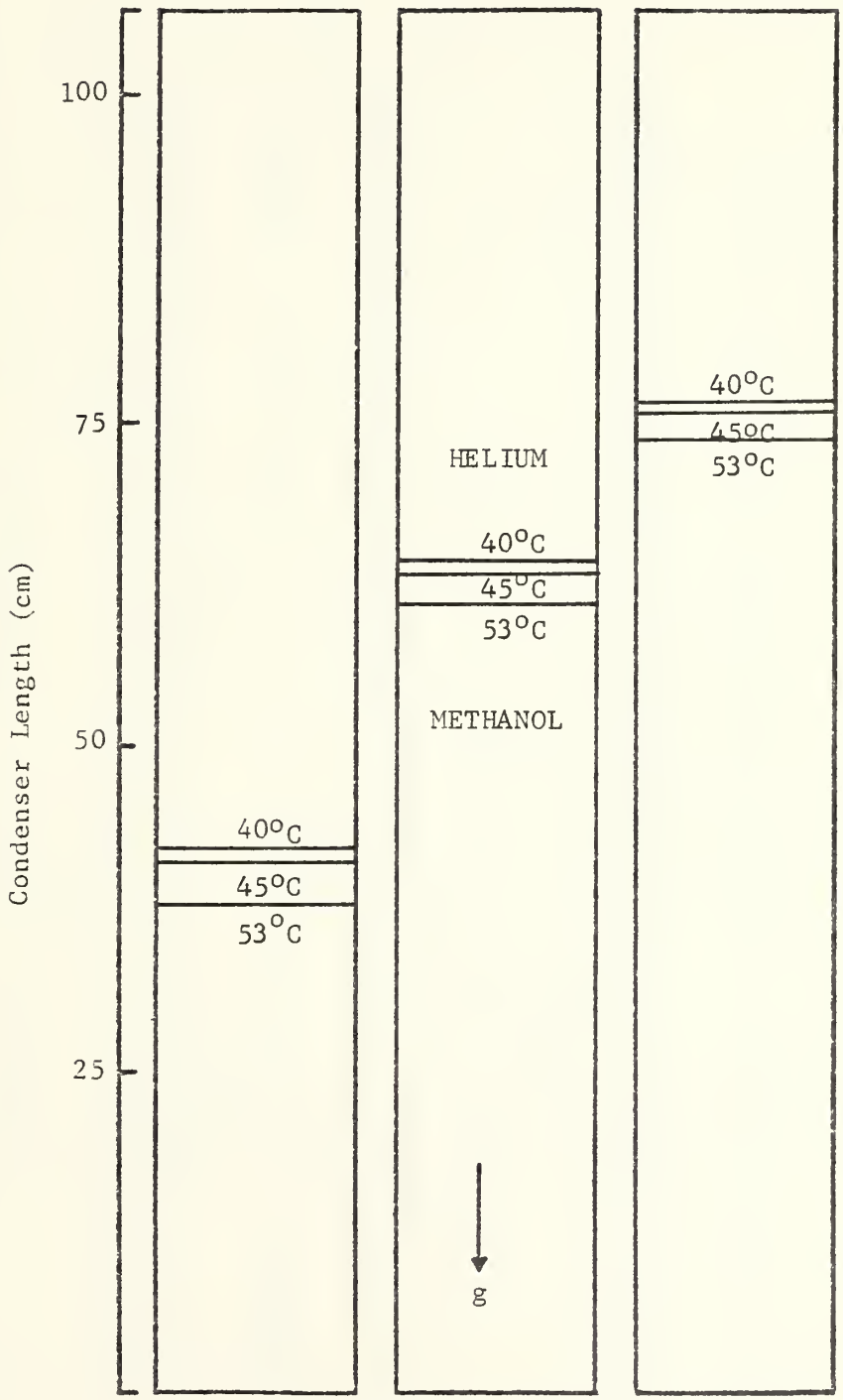

Liquid Crystal Isotherms - Vertical
3.05×10^{-5} kg Helium

Figure 23

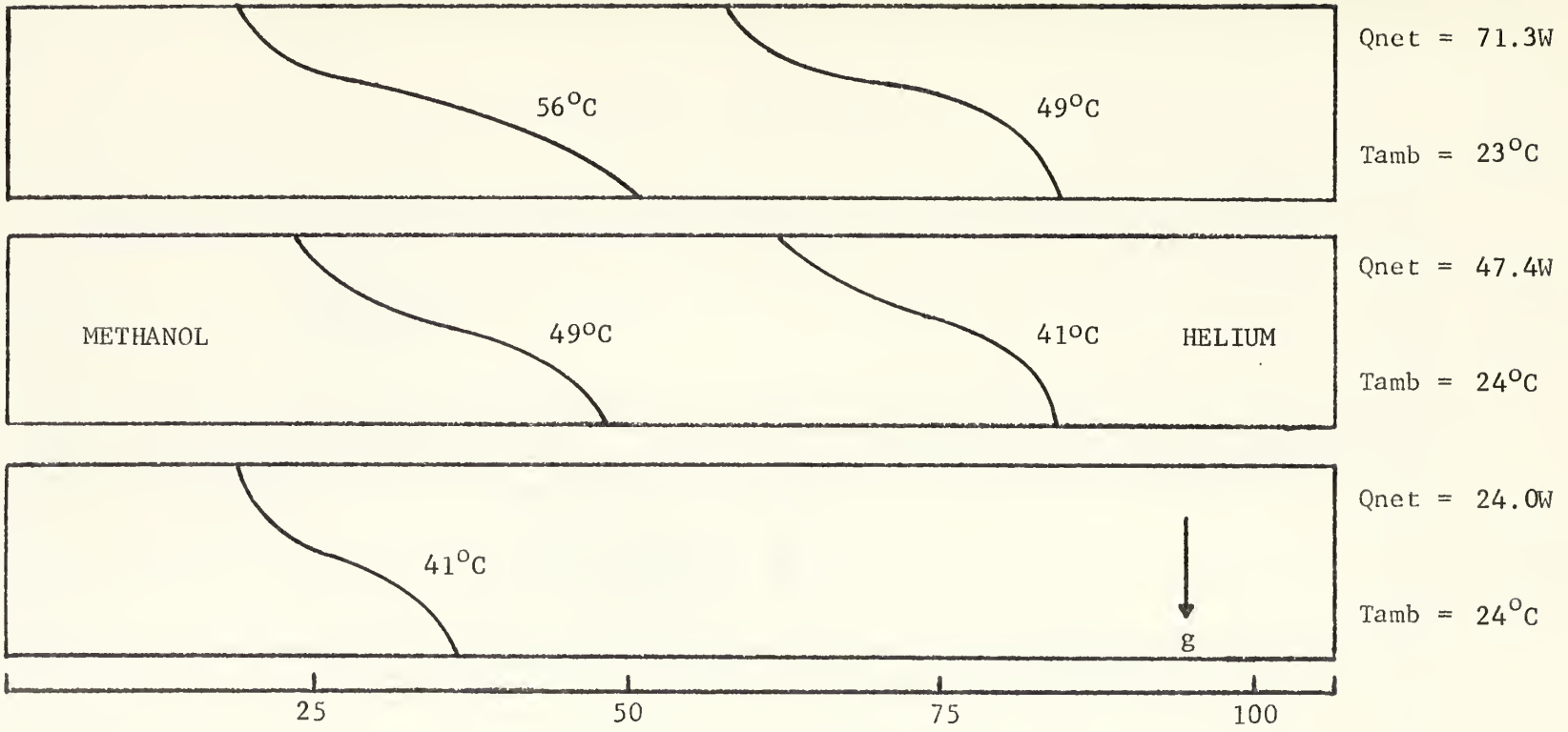

Liquid Crystal Isotherms - Horizontal - 1.82 x 10^{-4} kg Helium - Batts' Results

Figure 24

Qnet =	22.9W	46.6W	70.4W
Tamb =	23°C	24°C	25°C

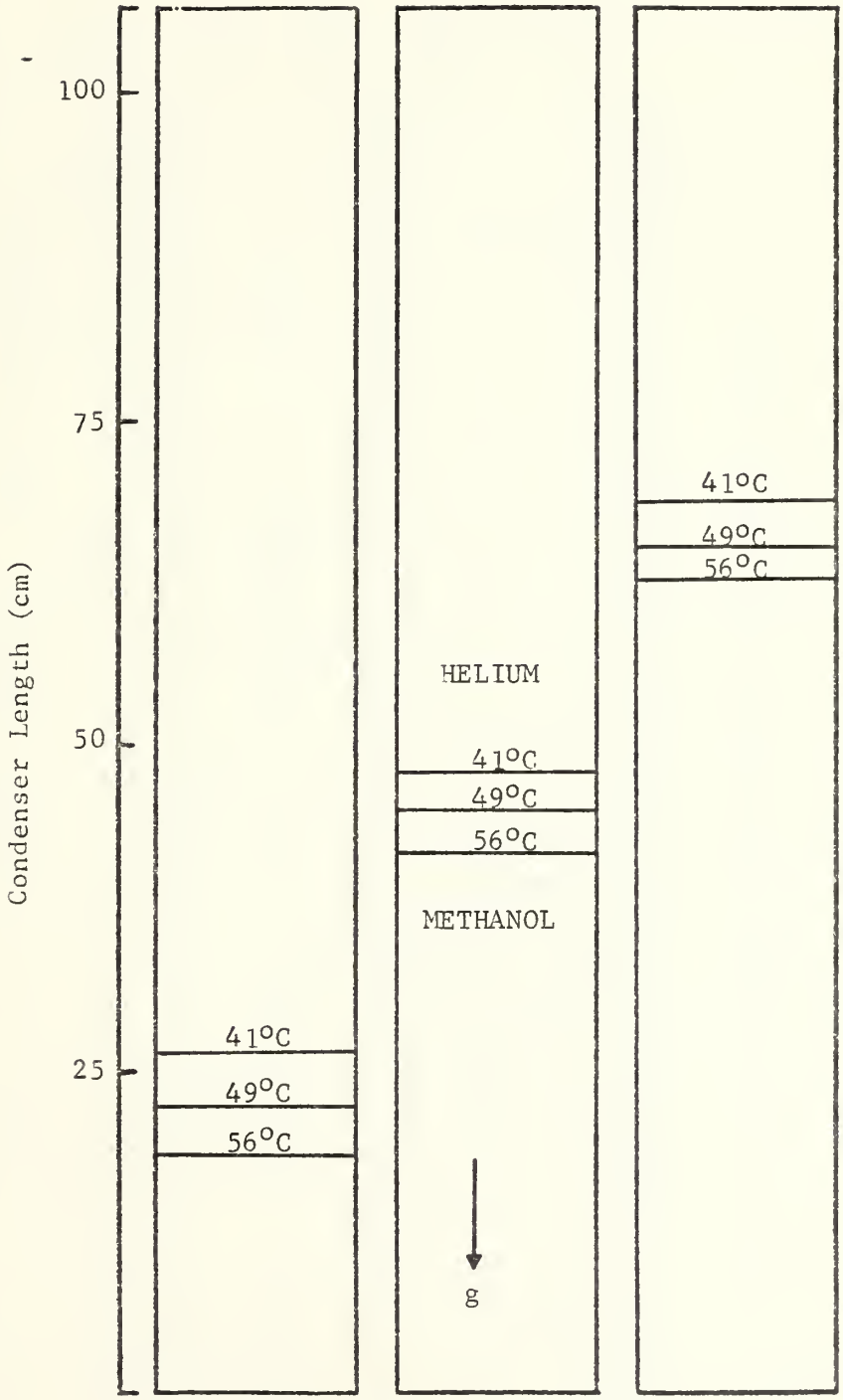

Liquid Crystal Isotherms - Vertical
1.82×10^{-4} kg Helium - Batts' Results

Figure 25

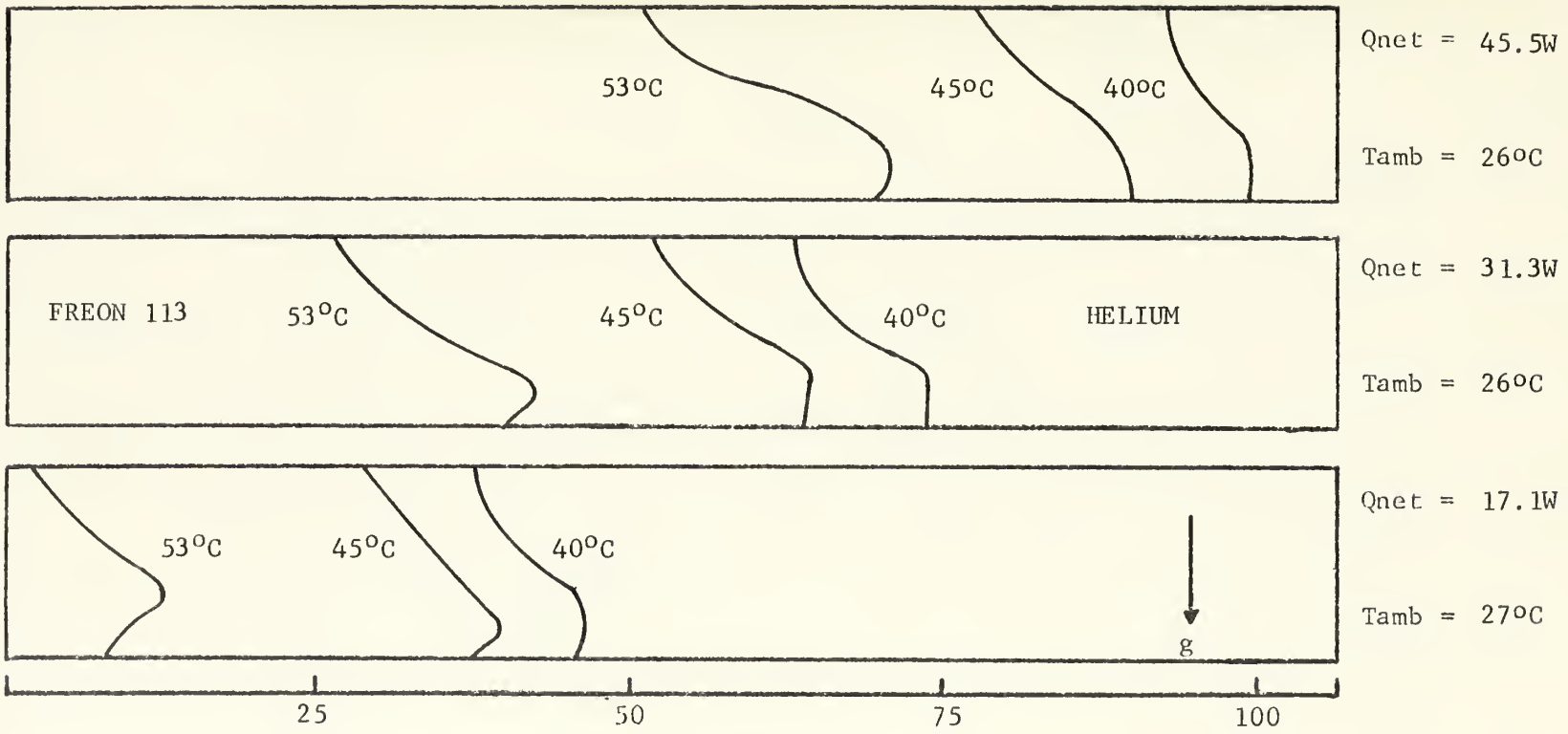

Liquid Crystal Isotherms - Horizontal - 1.42×10^{-4} kg Helium

Figure 26

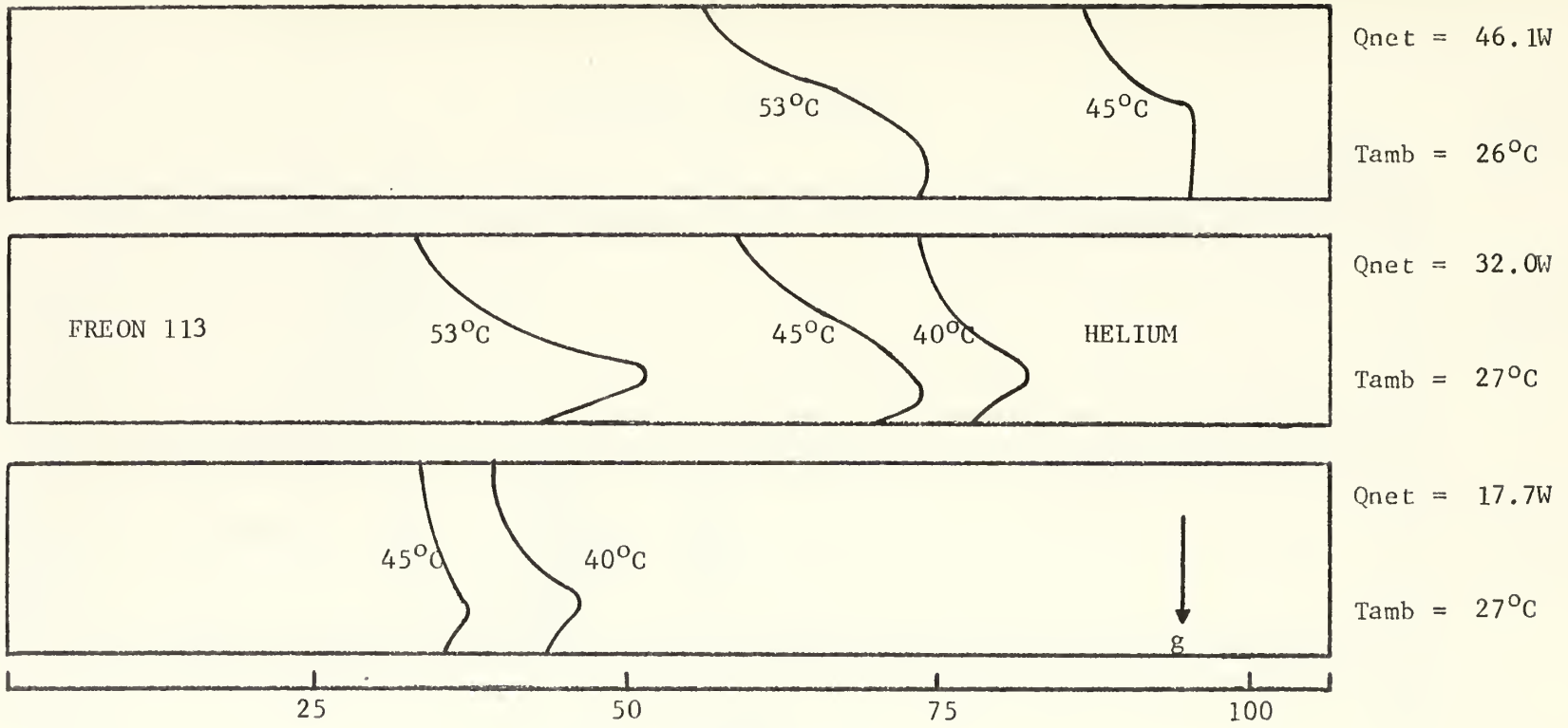

Liquid Crystal Isotherms - Horizontal - 8.26×10^{-5} kg Helium

Figure 27

Qnet =	17.4W	31.7W	46.4W
Tamb =	27°C	27°C	27°C

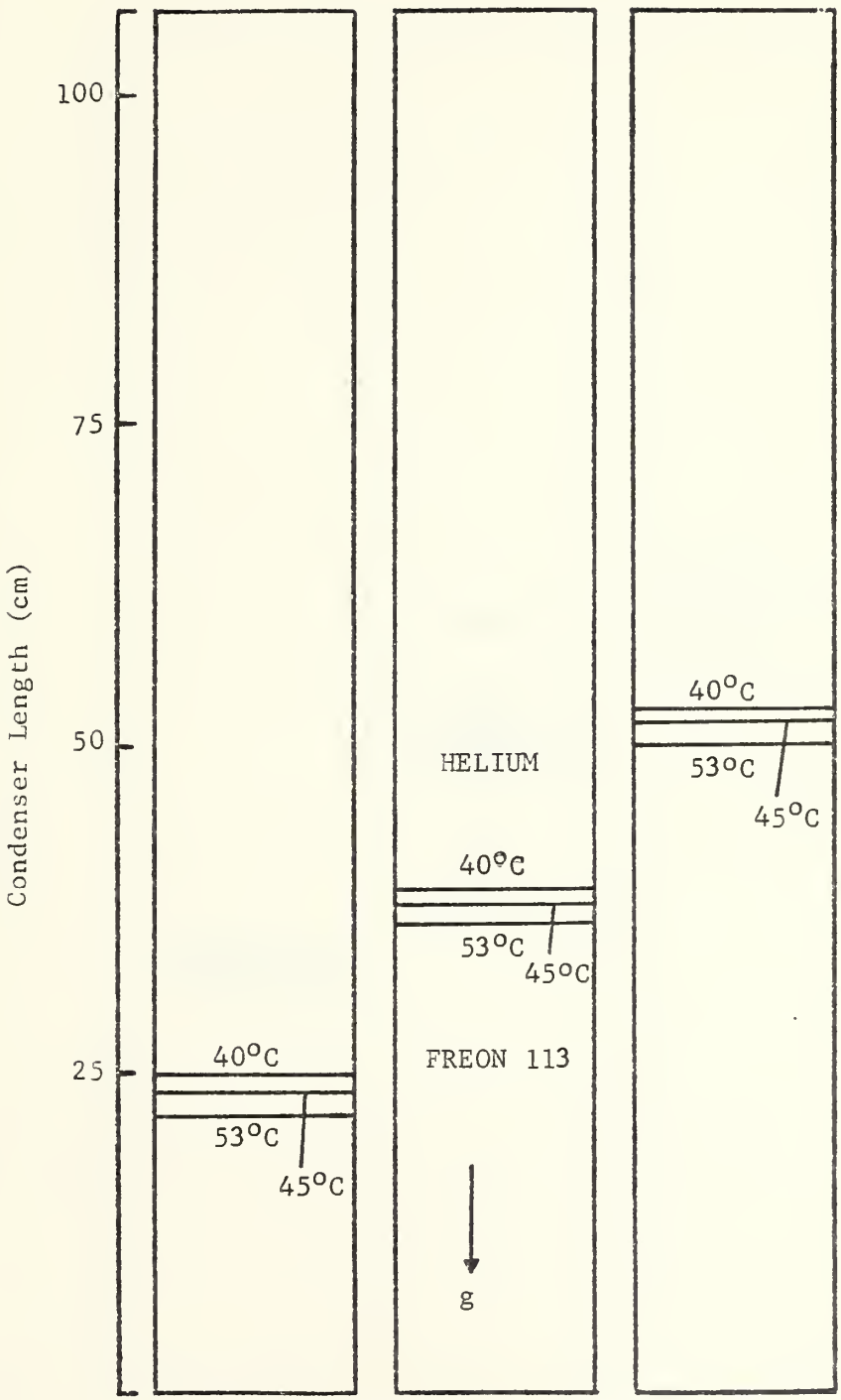

Liquid Crystal Isotherms - Vertical
1.42×10^{-4} kg Helium

Figure 28

Qnet =	18.0W	32.3W	46.8W
Tamb =	26°C	27°C	27°C

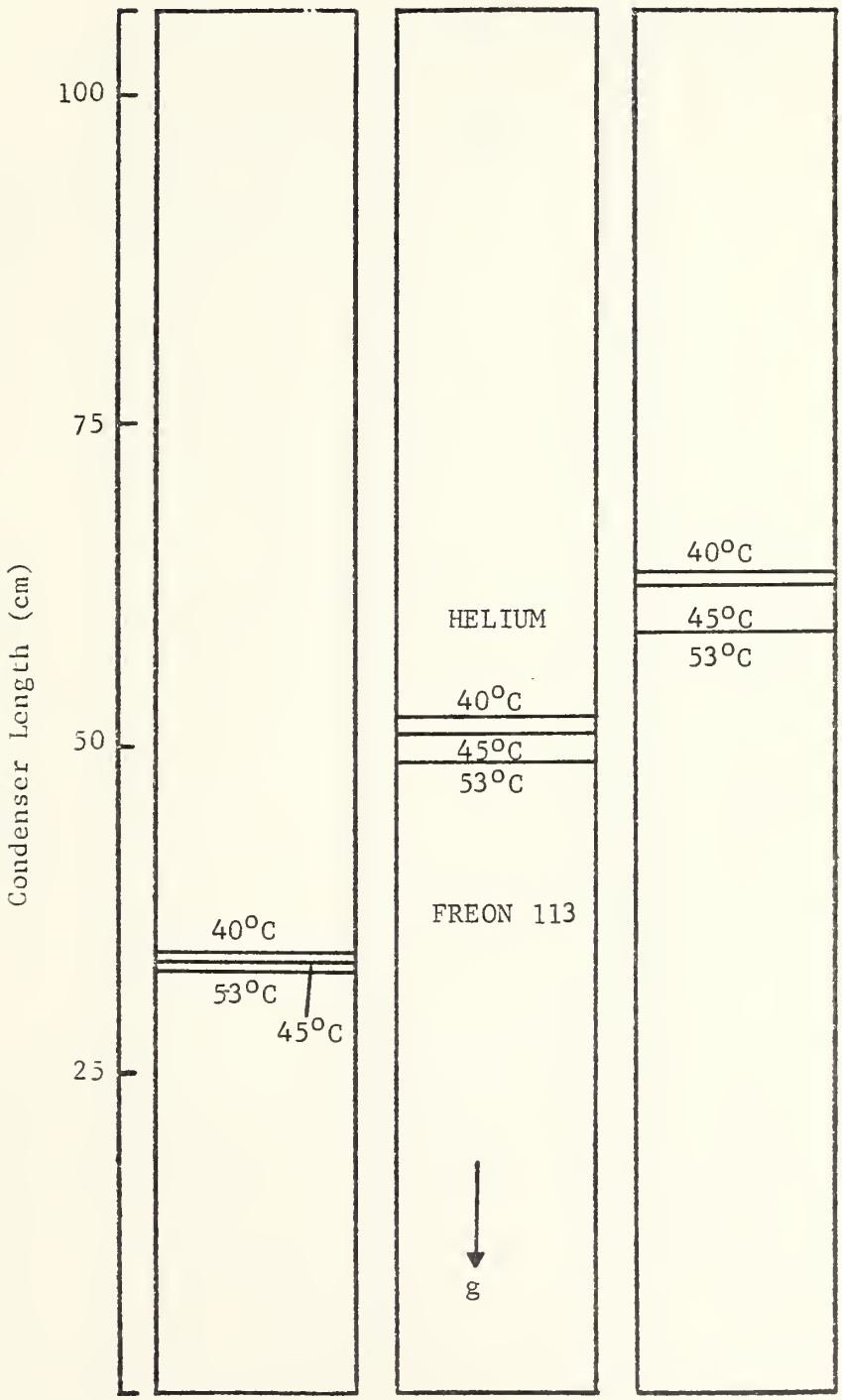

Liquid Crystal Isotherms - Vertical
8.26×10^{-5} kg Helium

Figure 29

Qnet =	19.0W	33.3W	50.4W
Tamb =	28°C	27°C	27°C

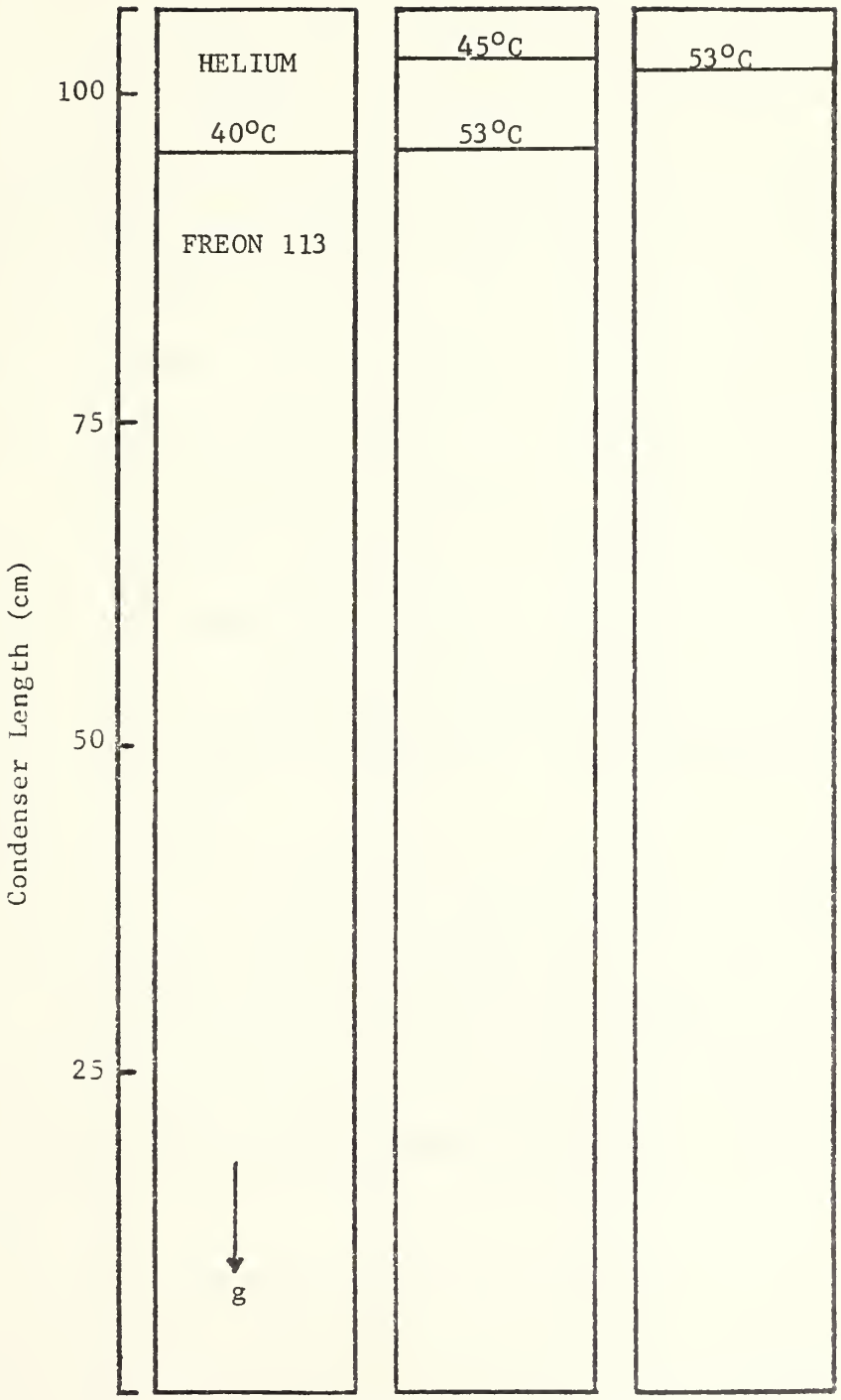

Liquid Crystal Isotherms - Vertical
4.72×10^{-6} kg Helium

Figure 30

the top to the bottom of the pipe. When the lighter helium gas was used, the helium concentrated along the top of the pipe with resulting lower temperatures in this region. With the heavier krypton as the non-condensible gas, the krypton formed a pool along the bottom of the heat pipe with the attendant lower temperatures. The conclusion from these liquid crystal isotherms is that gravitational effects caused the non-condensible gas concentration gradients which in turn caused the resulting temperature gradient perpendicular to the heat pipe axis.

Gravitational effects adequately explain why the Freon 113-helium liquid crystal isotherms, for the heat pipe in the horizontal position, were more horizontally oriented that the corresponding methanol-helium isotherms. Since the difference in molecular weights between Freon 113 and helium is significantly greater than for methanol and helium, gravitational forces should have a greater influence on the Freon 113-helium interface than on the methanol-helium interface. This premise is qualitatively confirmed by comparing the Freon 113-helium and methanol-helium isotherms.

The thermocouples along the top of the pipe were not useful in indicating the temperature gradient perpendicular to the heat pipe axis since these thermocouples can only show axial temperature gradients. Numerous thermocouples would have to be installed circumferentially in order to demonstrate this temperature gradient perpendicular to the heat pipe axis.

When the heat pipe was operated in the vertical position, the methanol-helium and Freon 113-helium heat pipe liquid crystal isotherms were much different than the isotherms for the methanol-krypton heat

pipe. The helium-loaded pipe isotherms indicated an axial temperature variation similar to that predicted by the diffuse front theory. In contrast, the temperature decreased progressively from the adiabatic section to the condenser end for the krypton-loaded pipe, and the liquid crystal isotherms were spaced much farther apart than for the helium-loaded heat pipes. These methanol-krypton heat pipe isotherms were not stationary, but rather they changed in a periodic manner with a frequency of approximately one cycle in 5 minutes and an amplitude of 6 to 7 cm. This oscillatory behavior indicates a gravitational instability (Rayleigh-Taylor) in this methanol-krypton interface. In this vertical position, the liquid crystals and thermocouples yielded compatible temperature data.

The influence of gravitational forces is reflected in the liquid crystal isotherms when the heat pipe was in the vertical position. The force which keeps the non-condensible gas in the condenser section is due primarily to the momentum of the vapor particles as they travel towards the condenser. The lighter helium gas quickly rose to the upper end of the pipe thus forming a plug which effectively prevented diffusion of the methanol vapor. However, the heavier krypton was affected by the stronger gravitational forces which oppose the momentum imparted to the krypton gas particles by the upward flow of the methanol vapor particles. As a result, there was a gradually increasing krypton gas concentration, although some methanol vapor did reach the condenser end.

Liquid crystals were used as an effective tool to observe qualitatively the isotherms. Near the end of the experiment, the brilliance

of the liquid crystal colors diminished over the 26-centimeter portion of the condenser nearest the adiabatic section. Since this particular section was usually at higher temperatures than the other areas of the condenser, it was concluded that high temperatures caused this reduced brilliance.

VI. SUMMARY

The experimental data show that when the molecular weights of the working fluid and non-condensible gas are significantly different, gravitational forces markedly influence the temperature gradient and orientation of the diffuse vapor-gas interface. Hence, the diffuse front theory should be modified by considering gravitational effects when designing a heat pipe for such vapor-gas combinations.

APPENDIX A

CALCULATION OF NET ABSORBED POWER

The net power absorbed by the heat pipe is assumed to be approximately equal to the power dissipated in the heater minus the insulation power loss. The temperature difference between thermocouples #97 and #91, which are located at different radial positions within the insulation, was used to calculate the insulation power loss.

$q\ (net) = q\ (htr) - q\ (loss)$

I. $q\ (htr) = V_1\ V_2\ /\ R$

V_1 = voltage drop across heater, volts

V_2 = voltage drop across series resistor, volts

R = series resistance (2.0236 ohms)

II. $$q\ (loss) = \frac{\Delta T}{\frac{\ln(r_2/\ r_1)}{2\pi\ KL}}$$

$\Delta T = T_{97} - T_{91}$

r_1 = radius to thermocouple #97 (2.5 cm)

r_2 = radius to thermocouple #91 (3.3 cm)

K = thermal conductivity of insulation (0.035 $\frac{w}{m\text{-}°C}$)

L = length of insulation (.34 m)

III. Sample Calculation for First Data Entry in Appendix C:

$V_1 = 28.09$ volts

$V_2 = 3.65$ volts

$\Delta T = 11.5°C$

$$q\ (net) = \frac{(28.09)\ (3.65)}{2.0236} - \frac{(11.5)(2)(3.14)(0.035)(.34)}{\ln\ (1.3)}$$

$$q\ (net) = 47.4 \text{ watts}$$

Appendix C summarizes the remaining experimental results.

APPENDIX B

CALCULATION OF NON-CONDENSIBLE GAS LOAD

The amount of non-condensible gas introduced into the heat pipe was calculated from data obtained at isothermal, ambient conditions.

$$m = \frac{(P_t - P_f)\ V\ M}{R\ T}$$

P_t = total pressure, n/m^2

P_f = working fluid partial pressure, n/m^2

V = heat pipe volume ($5.93 \times 10^{-4}\ m^3$)

M = molecular weight of non-condensible gas, g/gmole

R = universal gas constant (8.317 joule/gmole - °K)

T = pipe temperature, °K

Sample calculation for first krypton load of methanol-krypton heat pipe:

$P_t = 9.78 \times 10^4\ n/m^2$

$P_f = 1.81 \times 10^4\ n/m^2$

$T = 300$ °K

$M = 83.8$ g/gmole

$$m = \frac{[(9.78 - 1.81) \times 10^4]\ (5.93 \times 10^{-4})\ (83.8)}{(8.317)\ (300)}$$

$m = 1.59\ g = 1.59 \times 10^{-3}\ kg$

The other gas load results are listed in Table I.

APPENDIX C

SUMMARY OF DATA

I. Methanol is working fluid for following data

Position (Horizontal/ Vertical)	Type of Gas (Krypton/ Helium)	Amount of Gas (kg x 10,000)	Absorbed Power (Watts)	Evaporator Temp. (°C)	Condenser Temp. (°C)	Ambient Temp. (°C)
H	-	-	47.4	65	63	25
H	-	-	33.1	57	54	27
H	-	-	19.1	45	42	26
H	-	-	33.2	56	53	24
H	-	-	19.1	46	43	26
H	-	-	47.5	65	63	27
V	-	-	48.1	64	65	27
V	-	-	33.5	55	55	27
V	-	-	19.3	43	43	26
V	-	-	33.6	53	53	26
V	-	-	48.0	64	65	27
V	-	-	19.4	42	41	25
H	Kr	15.9	17.3	78	27	27
H	Kr	15.9	31.7	83	26	26
H	Kr	15.9	46.0	88	27	24
H	Kr	15.9	31.5	82	25	25
H	Kr	15.9	17.3	77	25	24
V	Kr	15.9	17.5	67	28	27

V	Kr	15.9	31.7	74	27	25
V	Kr	15.9	46.5	82	29	25
V	Kr	15.9	31.8	75	27	25
V	Kr	15.9	17.5	66	26	24
H	Kr	6.17	18.0	64	25	24
H	Kr	6.17	32.3	72	26	26
H	Kr	6.17	42.5	93	29	25
H	Kr	6.17	29.5	75	26	26
H	Kr	6.17	17.1	65	27	26
V	Kr	6.17	18.2	59	28	27
V	Kr	6.17	32.4	67	28	26
V	Kr	6.17	47.3	75	31	27
V	Kr	6.17	32.5	66	27	25
V	Kr	6.17	18.2	57	26	24
H	Kr	.055	19.2	47	34	24
H	Kr	.055	33.3	57	48	25
H	Kr	.055	43.5	85*	58	27
H	Kr	.055	29.6	64	43	24
H	Kr	.055	17.5	49	33	25
V	Kr	.055	19.2	47	42	28
V	Kr	.055	33.4	53	48	26
V	Kr	.055	47.9	64	62	26
V	Kr	.055	33.4	53	48	26
V	Kr	.055	19.2	45	39	26

APPENDIX C (Continued)

H	He	1.24	31.2	94	27	27
H	He	1.24	45.0	98	27	26
H	He	1.24	31.0	94	26	26
H	He	1.24	16.5	88	26	26
V	He	1.24	16.9	73	27	26
V	He	1.24	31.4	81	27	26
V	He	1.24	45.9	88	27	26
V	He	1.24	31.3	79	26	25
V	He	1.24	16.9	72	27	26
H	He	0.62	17.9	74	25	25
H	He	0.62	32.4	80	26	26
H	He	0.62	47.2	86	25	25
H	He	0.62	32.4	81	27	27
H	He	0.62	18.0	74	25	24
V	He	0.62	18.1	63	25	24
V	He	0.62	32.6	71	25	25
V	He	0.62	47.0	79	26	24
V	He	0.62	32.5	72	26	25
V	He	0.62	18.2	61	24	23
H	He	0.31	31.5	69	24	23
H	He	0.31	44.9	76	25	25
H	He	0.31	31.3	69	25	24
H	He	0.31	17.8	63	26	26

V	He	0.31	32.7	67	29	27
V	He	0.31	47.3	72	26	25
V	He	0.31	32.5	66	28	27
V	He	0.31	18.5	55	25	25

II. Freon 113 is working fluid for following data

H	-	-	33.4	53	52	26
H	-	-	47.3	62	62	26
H	-	-	33.2	52	51	25
H	-	-	19.2	41	39	25
V	-	-	33.4	53	46	25
V	-	-	47.8	61	61	24
V	-	-	33.3	55	46	27
V	-	-	19.1	41	32	24
H	He	1.42	31.4	90	33	28
H	He	1.42	45.5	96	42	26
H	He	1.42	31.3	89	31	26
H	He	1.42	17.1	81	27	27
V	He	1.42	31.7	82	28	28
V	He	1.42	46.4	92	28	27
V	He	1.42	31.7	83	28	27

APPENDIX C (Continued)

V	He	1.42	17.4	71	28	27
V	He	.047	33.3	55	43	27
V	He	.047	47.6	65	53	27
V	He	.047	33.3	55	42	27
V	He	.047	19.0	45	33	28
H	He	.047	33.0	55	51	27
H	He	.047	47.0	62	59	26
H	He	.047	33.0	53	49	25
H	He	.047	18.9	45	39	28
H	He	0.83	32.0	79	35	27
H	He	0.83	46.1	86	45	26
H	He	0.83	17.7	71	28	27
V	He	0.83	18.0	63	27	26
V	He	0.83	32.3	76	27	27
V	He	0.83	46.8	83	28	27

LIST OF REFERENCES

1. Barsch, W. O., and Winter, E. R. F., "The Heat Pipe," Advances in Heat Transfer, v. 7, Irvine, T. F., and Hartnett, J. P., Eds., Academic Press, 1971.

2. Gaugler, R. S., Heat Transfer Devices, U. S. Patent 2,350,348, 21 December 1942.

3. Grover, G. M., Cotter, T. P., and Erickson, G. F., "Structures of Very High Thermal Conductance," Journal of Applied Physics, v. 35, p. 1990, 1964.

4. Dunn, P. D., and Reay, D. A., Heat Pipes, Pergamon Press, 1976.

5. Chi, S. W., Heat Pipe Theory and Practice, McGraw-Hill Book Co., 1976.

6. NASA Contract Report 2018, Theory and Design of Variable Conductance Heat Pipes, by B. D. Marcus, April 1972.

7. Bienert, W., "Heat Pipes for Temperature Control," presented at Intersociety Energy Conversion Engineering Conference, Washington, D. C., 1969.

8. Rohani, A. R., and Tien, C. L., "Steady Two-Dimensional Heat and Mass Transfer in the Vapor-Gas Region of a Gas-Loaded Heat Pipe," ASME Paper No. 72-WA/HT-34, 1972.

9. Naydan, T. P., Investigation of a Variable Conductance Heat Pipe, M. S. Thesis, Naval Postgraduate School, 1975.

10. Batts, W. H., Investigation of Gravitational Effects on a Variable Conductance Heat Pipe Utilizing Liquid Crystal Thermography, M. S. Thesis, Naval Postgraduate School, 1975.

11. Humphreys, W. I., Investigation of Gravitational Effects on the Performance of a Variable Conductance Heat Pipe, M. S. Thesis, Naval Postgraduate School, 1973.

12. Cooper, T. E., Field, R. J., and Meyer, J. F., "Liquid Crystal Thermography," Journal of Heat Transfer, Trans. ASME, v. 97, Series C, No. 3, pp. 442-450, August 1975.

INITIAL DISTRIBUTION LIST

		No. Copies
1.	Defense Documentation Center Cameron Station Alexandria, Virginia 22314	2
2.	Library, Code 0142 Naval Postgraduate School Monterey, California 93940	2
3.	Department Chairman, Code 69 Department of Mechanical Engineering Naval Postgraduate School Monterey, California 93940	2
4.	Assoc. Professor M. D. Kelleher, Code 69Kk Department of Mechanical Engineering Naval Postgraduate School Monterey, California 93940	1
5.	LT Robert S. Owendoff, USN 11156 Byrd Drive Fairfax, Virginia 22030	1

Thesis
0953
c.1

169602

Owendoff
Gravitational effects on the operation of a variable conductance heat pipe.